JACS
JOURNAL OF THE AMERICAN CHEMICAL SOCIETY
pubs.acs.org/JACS
Article

Molecular Complexity-Inspired Synthetic Strategies toward the Calyciphylline A-Type *Daphniphyllum* Alkaloids Himalensine A and Daphenylline

Brandon A. Wright, Taku Okada, Alessio Regni, Guilian Luchini, Shree Sowndarya S. V, Nattawadee Chaisan, Sebastian Kölbl, Sojung F. Kim, Robert S. Paton,* and Richmond Sarpong*

Cite This: *J. Am. Chem. Soc.* 2024, 146, 33130−33148

ABSTRACT: In this report, we detail two distinct synthetic approaches to calyciphylline A-type *Daphniphyllum* alkaloids himalensine A and daphenylline, which are inspired by our analysis of the structural complexity of these compounds. Using MolComplex, a Python-based web application that we have developed, we quantified the structural complexity of all possible precursors resulting from one-bond retrosynthetic disconnections. This led to the identification of transannular bonds as especially simplifying to the molecular graph, and, based on this analysis, we pursued a total synthesis of himalensine A from macrocyclic intermediates with planned late-stage transannular ring formations. Despite initial setbacks in accessing an originally designed macrocycle, targeting a simplified macrocycle ultimately enabled investigation of this intermediate's unique transannular reactivity. Given the lack of success to access himalensine A based solely on molecular graph analysis, we revised our approach to the related alkaloid, daphenylline. Herein, we also provide the details of the various synthetic challenges that we encountered and overcame en route to a total synthesis of daphenylline. First, optimization of a Rh-mediated intramolecular Buchner/6π-electrocyclic ring-opening sequence enabled construction of the pentacyclic core. We then describe various attempts to install a key quaternary methyl group and, ultimately, our solution to leverage a [2 + 2] photocycloaddition/bond cleavage sequence to achieve this elusive goal. Finally, a late-stage Friedel−Crafts cyclization and deoxygenation facilitated the 11-step total synthesis, which was made formally enantioselective by a Rh-mediated dihydropyridone conjugate arylation. Complexity analysis of the daphenylline synthesis highlights how complexity-building/C−C cleavage combinations can be uniquely effective in achieving synthetic outcomes.

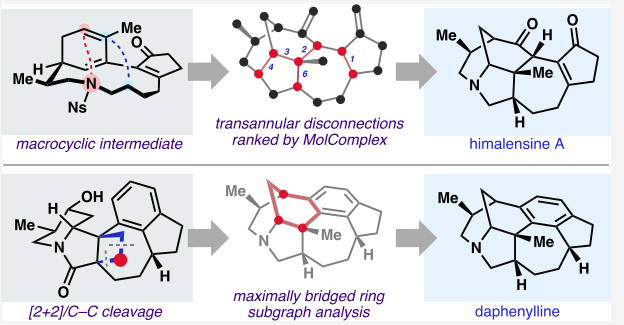

1. INTRODUCTION

Retrosynthetic analysis is generally guided by disconnections that result in the greatest reduction in structural complexity.[1] This principle, originally proposed by Corey and Wipke for the development of the computer-based retrosynthesis algorithm LHASA[2] (Logic and Heuristics Applied to Synthetic Analysis), has since found broad application as a fundamental heuristic in retrosynthesis planning. Complex synthetic targets can be iteratively reduced, through retrosynthetic analysis, to simpler intermediates, which are either commercially available or have been previously reported.

However, in most cases, the evaluation of molecular complexity in retrosynthetic analysis is performed intuitively and qualitatively. Although human intuition can perform consistently on aggregate, an individual chemist's judgment of molecular complexity can be subject to variations in perception and pattern recognition.[3] On the other hand, methods for scoring structural complexity, such as that of Bertz,[4] Böttcher,[5] and Waldmann et al.,[6] have found application in evaluating the relative merits of synthetic approaches to natural product targets.[7,8] These metrics offer an attractive means to reliably quantify structural complexity and thus might serve as a source of inspiration for guiding retrosynthetic disconnections.[4,9,10]

Our laboratory has had a longstanding interest in how computer-guided analyses might aid in synthesis planning of complex targets. Enabled by MaxBridge,[11] identification of the maximally bridged ring through network analysis has served as an inspirational starting point for the development of efficient synthetic strategies toward a number of natural products.[12−15] In an effort to expand this complexity analysis beyond the maximally bridged ring heuristic, we became intrigued by the possibility that complexity metrics might drive new advances in

Received: August 29, 2024
Revised: November 2, 2024
Accepted: November 8, 2024
Published: November 20, 2024

https://doi.org/10.1021/jacs.4c11252
J. Am. Chem. Soc. 2024, 146, 33130−33148

synthetic strategies. By virtue of their complex, polycyclic molecular architectures, broad structural diversity, and rich history in the field of synthetic chemistry, the *Daphniphyllum* alkaloids presented an attractive opportunity for investigating these strategies.

The *Daphniphyllum* alkaloids are a structurally diverse collection of natural products isolated from evergreen shrubs and trees found throughout East Asia, Southeast Asia, and the Indian subcontinent. Since the isolation of the first *Daphniphyllum* alkaloid in 1826,[16] vastly different skeletal frameworks within this class of natural products have since been identified (Figure 1A).[17−20] Seminal contributions to the total syntheses of these alkaloids from Heathcock[21−23] paved the way for more recent contributions from Carreira and Weiss,[24] Smith and Shvartsbart,[25,26] Hanessian et al.,[27] Li et al.,[28,29] Fukuyama et al.,[30] Dixon et al.,[31,32] Xu et al.,[33−35] Zhai et al.,[36] Li et al.,[37] Li et al.,[38,39] Lu et al.,[40] Yang et al.,[41] and our laboratory among others.[42−44]

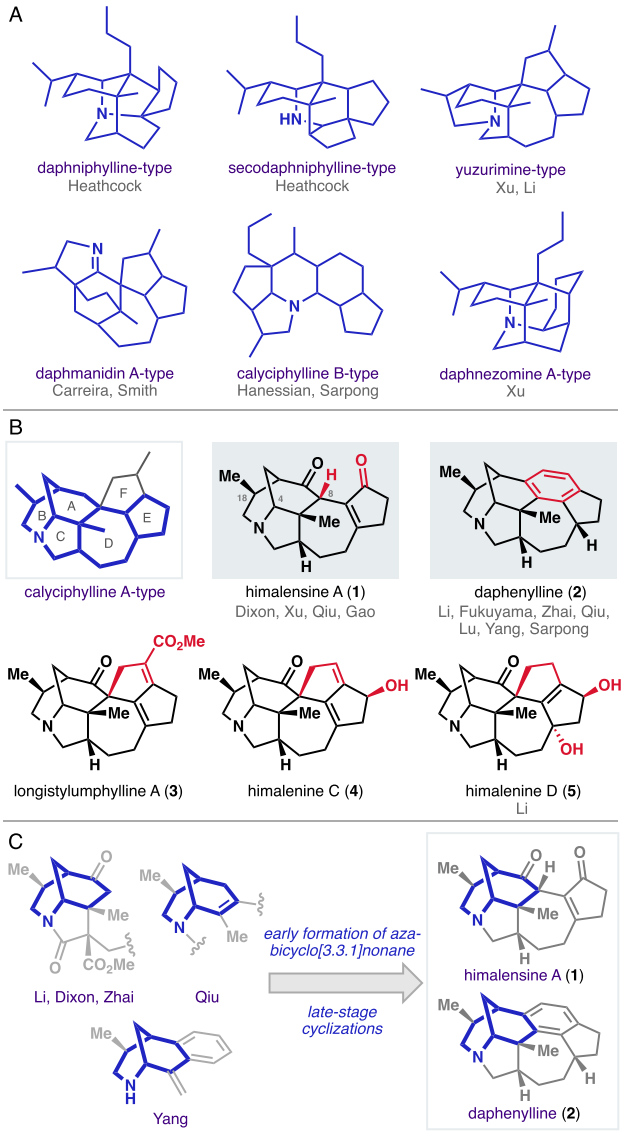

Figure 1. (A) Selected skeletal frameworks of the major subclasses of *Daphniphyllum* alkaloids. (B) Recently isolated *Daphniphyllum* alkaloids containing simplified, hydroxylated, and rearranged calyciphylline A-type carbon skeletons. (C) Previous approaches to the calyciphylline A-type scaffold from bicyclic or tricyclic intermediates.

Since the isolation of calyciphylline A,[45] over 50 calyciphylline A-type *Daphniphyllum* alkaloids have been reported, making these congeners the largest subclass within this family of alkaloids (Figure 1B).[17,19,46] Several of these newly reported calyciphylline A-type alkaloids feature slight structural variations on the eponymous structural subclass. For example, himalensine A (**1**), isolated in 2016 from *Daphniphyllum himalense* by Yue and co-workers,[47] lacks the F-ring and a quaternary carbon at C8. Daphenylline (**2**), isolated from the fruits of *Daphniphyllum longeracemosum* in 2009 by Hao et al.,[48] bears a unique benzene-fused ring embedded within the calyciphylline A-type framework. While compounds such as longistylumphylline A (**3**)[49] contain the full calyciphylline A framework, more oxidized variants have also been identified: himalenine C (**4**) and himalenine D (**5**), isolated by Yue et al. in 2015,[50] contain additional sites of hydroxylation on the E-ring.

With himalensine A (**1**) and daphenylline (**2**) as representative calyciphylline A-type congeners, we envisioned that development of efficient syntheses of these targets might enable a unified approach to other *Daphniphyllum* alkaloids of even greater structural complexity. Previous approaches to **1**[31−33,51] and **2**[28,36,41,52] have largely centered on the initial construction of the complex aza-bicyclo[3.3.1]nonane-containing bicyclic or tricyclic core, which is then elaborated by a series of late-stage cyclizations to complete the polycyclic framework (Figure 1C). Although facile access to the aza-bicyclo[3.3.1]nonane core represents a noteworthy milestone toward the calyciphylline A-type skeleton, late-stage challenges in the oxidation strategy and functional group manipulations can arise from the emergent properties[53] of these complex intermediates, increasing the number of total steps required to complete these syntheses. With the valuable insights gained from these previous efforts, we reasoned that late-stage generation of the complex aza-bicyclo[3.3.1]nonane core could address these hurdles.

2. RESULTS AND DISCUSSION

2.1. Initial Synthesis Strategy of Himalensine A. The development of our approach to himalensine A (**1**) began with complexity analysis of the calyciphylline A-type scaffold (Figure 2A). Considering the all-carbon skeletal framework as a molecular graph, a series of theoretical one-bond disconnections generated 24 possible precursors which were scored according to Bertz's C_T score[4] (see the Supporting Information for full details). In this retrosynthetic analysis, the proposed disconnections were then ranked according to the scored reduction in structural complexity. Here, an intriguing trend rose to the fore: five of the seven top-ranked precursors involved breaking a *transannular* bond, suggesting that these types of disconnections are maximally simplifying to the polycyclic calyciphylline A-type framework. While our complexity analysis was originally performed manually, we later developed a Python-based web application, MolComplex (www.molcomplex.org), which can carry out this entire complexity scoring workflow in an automated fashion (see the Supporting Information for full details). Additionally, since MolComplex ranks disconnections solely according to the simplification of the molecular graph, no chemical reactivity is explicitly considered, leaving wide latitude for the expert user to devise creative implementations of these strategies.

https://doi.org/10.1021/jacs.4c11252
J. Am. Chem. Soc. 2024, 146, 33130−33148

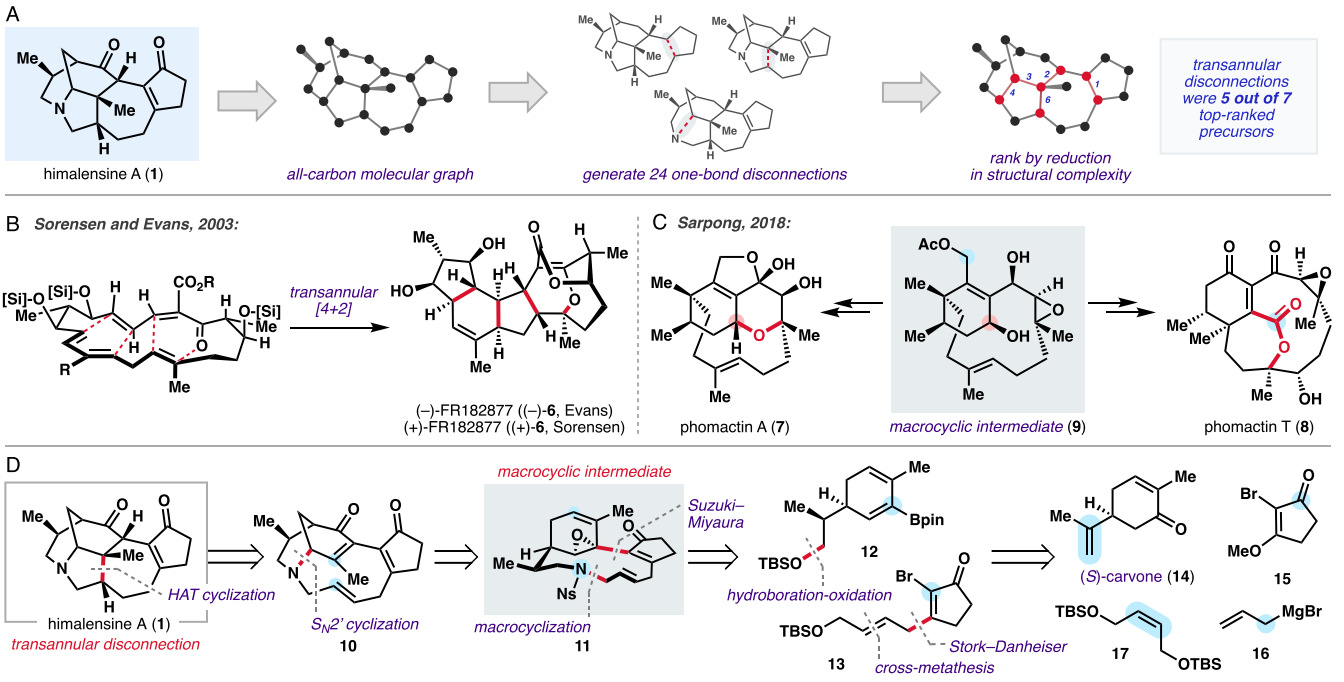

Figure 2. (A) Complexity analysis workflow with MolComplex. (B) Sorensen and Evans' transannular approaches to FR281877 (**6**). (C) Synthesis of phomactins A (**7**) and T (**8**) from a common macrocyclic intermediate (**9**). (D) Retrosynthesis of himalensine A (**1**) involving transannular disconnections.

Scheme 1. Synthesis of Fragments 12 and 13 and Observed Cross-Coupling Challenges

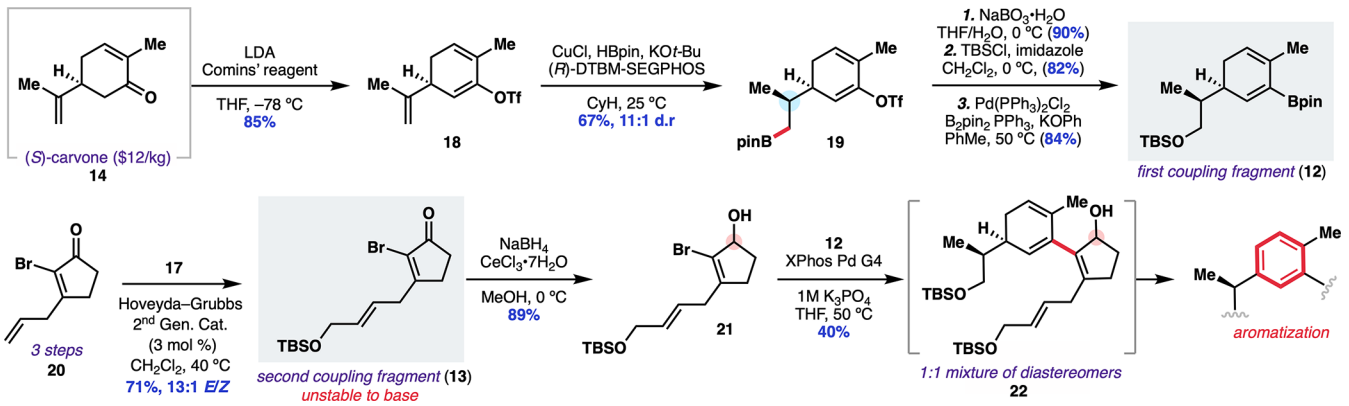

This analysis was found to be in agreement with the study by Bertz and Sommer,[9] who showed that related N_S and N_T complexity scores identified transannular bonds as maximally simplifying to bicyclic molecular graphs. Despite MolComplex's alignment with previous work on simplification of molecular graphs, prevailing synthetic heuristics established by Corey and Cheng[1] explicitly warn against transannular disconnections due to the inherent synthetic challenge of building the corresponding macrocyclic precursor. However, in the decades since Corey's codification of retrosynthesis rules, advances in synthetic methodology have enabled the reliable construction of macrocycles across a range of natural product scaffolds.[54−56] Inspired by examples such as Sorensen and Evans' transannular approaches to FR182877 (**6**, Figure 2B),[57,58] and in view of our previous synthesis of phomactin terpenoids A (**7**) and T (**8**) from a common macrocyclic intermediate (**9**, Figure 2C),[59] we became enticed by the general approach of using macrocycles as strategic linchpins for the construction of complex, polycyclic scaffolds.

On the basis of this analysis, we chose to pursue a transannular strategy for the synthesis of himalensine A (**1**). Our retrosynthesis began with the sequential disconnection of two transannular bonds across the central pyrrolidine core (Figure 2D). In the first disconnection, we planned a hydrogen atom transfer (HAT)-initiated transannular Giese-type addition[60] into the enone moiety in 10-membered macrocycle **10** to form the final C−C bond. In turn, we envisioned **10** could arise through transannular S_N' cyclization with the vinyl epoxide in **11** upon *N*-deprotection. We reasoned that, aided by the preorganization afforded by macrocycle **11**'s restricted conformation, these ambitious transannular cyclizations would give rise to the calyciphylline A-type skeleton in the forward sense. In turn, 12-membered macrocycle **11** could arise in a convergent fashion by Mitsunobu macrocyclization and Suzuki−Miyaura cross-coupling from boronate ester **12** and cyclopentenone **13**. Boronate ester **12** could ultimately be constructed through stereoselective hydroboration and oxidation of the isopropenyl unit in (*S*)-carvone (**14**), a readily

https://doi.org/10.1021/jacs.4c11252
J. Am. Chem. Soc. 2024, 146, 33130−33148

available enantioenriched starting material. Finally, cyclopentenone **13** could be prepared in parallel by Stork–Danheiser alkylation of vinylogous ester **15** with vinyl magnesium bromide (**16**) followed by extension of the alkyl chain by cross-metathesis with **17**.

2.2. Synthetic Efforts toward Himalensine A. *2.2.1. Synthesis of the Key Macrocyclic Intermediate.* Efforts to access alkene-bearing macrocyclic **11** began with the preparation of a suitable cyclohexadiene cross-coupling fragment from (*S*)-carvone (**14**, Scheme 1). We envisioned that cross-coupling handles such as a vinyl triflate or a boronic ester could be accessed from the enone carbonyl in **14**, and hydrofunctionalization of the isopropenyl unit would accomplish both the setting of the methyl-bearing stereocenter and provide a functional handle for eventual installation of the requisite amine. Initial attempts to hydroborate (*S*)-carvone (**14**) were met with challenges. Previous work from Overman et al.[61,62] had established that treatment of **14** with 9-BBN proceeds without diastereoselectivity at the 1,1-disubstituted alkene, requiring a lengthy sequence to epimerize the methyl group. Given the lack of substrate control, we were drawn to catalyst-controlled methods using Cu(I)-H species as reported by Yun et al.[63] Application of these conditions, however, to **14** resulted only in decomposition, presumably due to deleterious reactivity of the nucleophilic Cu–H species with the enone. To address this issue, we reasoned that formation of the cross-coupling handle upfront would effectively mask the enone's electrophilicity. To this end, treatment of (*S*)-carvone (**14**) with LDA and Comins' reagent[64] afforded vinyl triflate **18** in excellent yield. Cu(I)-mediated hydroboration of **18** proceeded smoothly with (*R*)-DTBM SEGPHOS as the ligand to give pinacol boronic ester **19** in good yields and diastereoselectivity (6:1 d.r.). Given that (*S*)-DTBM SEGPHOS affords the opposite diastereomer in 13:1 d.r., we believe this transformation is catalyst-controlled. With insights from Hartwig and Xi,[65] the diastereoselectivity could be improved to 11:1 d.r. (or 20:1 with (*S*)-DTBM SEGPHOS) with cyclohexane as solvent.

Having established the methyl-bearing stereocenter from the isopropenyl unit, we accessed the targeted cross-coupling fragment in a three-step sequence. First, mild oxidation of the pinacol boronic ester group with $NaBO_3 \cdot H_2O$, followed by protection of the resulting hydroxy group as the TBS-ether and conversion of the electrophilic vinyl triflate moiety to a cross-coupling boron-based nucleophile with Miyaura borylation conditions[66] afforded vinyl pinacol boronic ester **12**, the first targeted fragment.

The cyclopentenone fragment (**13**, Scheme 1) was synthesized from known cyclopentenone **20**. This was achieved in a known three-step sequence[67] from 1,3-cyclopentane dione by bromination at the 2-position, vinylogous methyl ester formation, and Stork–Danheiser alkylation of the resulting cyclopentenone (**15**) with allyl magnesium bromide (**16**) gave allyl cyclopentenone **20** upon acidic hydrolysis. Installation of the alkene-containing side chain was achieved through cross-metathesis[68] with 1,4-*cis*-butene diol-derived **17** to selectively give **13**, predominantly as the (*E*)-isomer. At this stage, Suzuki–Miyaura cross-coupling with **12** was attempted; however, rapid decomposition of **13** was observed upon exposure to base, impeding productive coupling. Mitigation of this deleterious reactivity was achieved through Luche-reduction of enone **13** to allyl alcohol **21**, which, when subjected to identical Suzuki–Miyaura coupling conditions, gave dendralene **22** as a 1:1 mixture of diastereomers. Unfortunately, this success was short-lived: spontaneous aerobic oxidation of the cyclohexadiene fragment to the corresponding arene was observed upon isolation and storage, further complicating this approach.

Given the hurdles faced in the synthesis of macrocycle **11**, which contained sites of activation for subsequent transannulation, we further revised our approach to target macrocycle **23** (Figure 3A) bearing a simple alkyl chain.

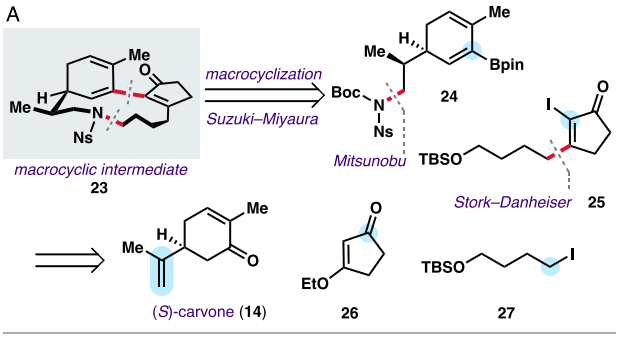

entry	conditions	conversion[a]	yield[b]	scale
1	CuCl (5%), L (5.5%)	67–85%	67%	250 mg
2	CuCl (1%), L (1.1%)	18%	n.d.	250 mg
3	CuCl (10%), L (1%)	55%	n.d.	250 mg
4	CuCl (10%), L (1%), PPh_3 (5%)	84%	n.d.	250 mg
5	**CuCl (10%), L (1.5 %), PPh_3 (5%)**	**>90%**	**77%**	**10 g**
6	**CuCl (10%), L (1.5 %), PPh_3 (5%)**	**>90%**	**78%**	**35 g**

L = (*R*)-DTBM SEGPHOS

Figure 3. (A) Revised retrosynthesis targeting simplified macrocyclic intermediate **23**. (B) Optimization of copper(I)-mediated stereoselective hydroboration of **28**. [a]Conversion ratios were measured by ^{1}H NMR. [b]All yields refer to isolated yield. n.d. = not determined.

Despite the fact that **23** would lack reactive sites for transannular bond formation, we reasoned that this synthetically simpler approach would allow us to probe the reactivity of the macrocycle and explore late-stage oxidation tactics to promote transannulation. Access to **23**, we envisioned, could be achieved by macrocyclization and Suzuki–Miyaura coupling from fragments **24** and **25** which, in turn, could be prepared by analogy to **12** and **13**.

Realization of this revised strategy required revisiting the Cu-mediated hydroboration of (*S*)-carvone triflate **18**, which proceeded only to low conversions on scales greater than 250 mg (Figure 3B). At this stage, we found that vinyl nonaflate **28** (prepared in one step from **14**) displayed superior stability against aerobic oxidation to the arene. On scale, a practical limitation also arose: large quantities of (*R*)-DTBM SEGPHOS is cost-prohibitive ($142/g from STREM). Lowering the catalyst loadings to 1 mol % proved detrimental to the overall conversion (Figure 3B, entry 2). Noting from mechanistic ^{31}P NMR studies from Hartwig and Xi[65] that the majority of ligand remains free in solution, we increased Cu-loadings as a cost-effective way to boost concentrations of

https://doi.org/10.1021/jacs.4c11252
J. Am. Chem. Soc. 2024, 146, 33130–33148

Scheme 2. Cross-Coupling of Cyclohexadiene 24 and Cyclopentenone 25 and Preparation of Macrocyclic Intermediate 23 and Formation of Ketoepoxide 31 Mitigating Undesired Overoxidation and Aromatization

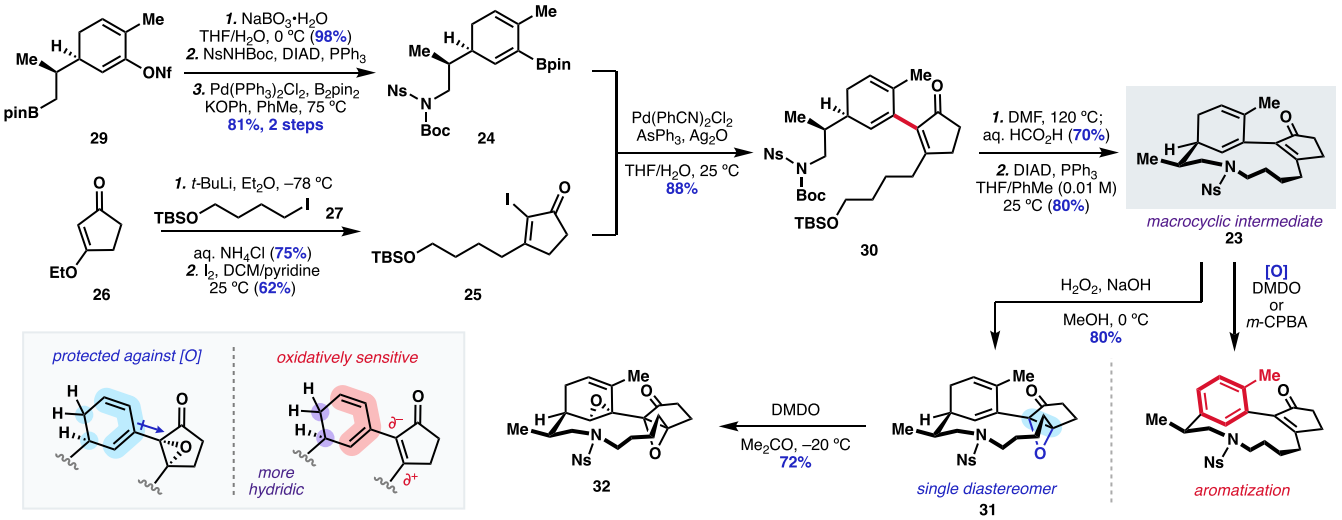

active, ligated Cu–H (55% conversion, entry 3). Inclusion of PPh_3 as a nonparticipating ancillary ligand[69] further improved conversion to 84% (entry 4) with no loss in diastereoselectivity. Slightly modified conditions could be conducted on decagram scale with no loss in efficiency (77–78% yield, entries 5 and 6).

With access to large quantities of **29**, we turned our attention to synthesis of the cross-coupling fragments (Scheme 2). Oxidation of **29** with $NaBO_3 \cdot H_2O$ smoothly gave the corresponding alcohol in nearly quantitative yield. Mitsunobu amination, followed by Miyaura borylation,[66] afforded vinyl boronate ester **24** in 81% yield over two steps. In parallel, cyclopentenone **25** was prepared from cyclic vinylogous ester **26** in a two-step sequence. First, Stork–Danheiser alkylation with the corresponding alkyllithium species derived from alkyl iodide **27** afforded the 3-substituted cyclopentenone in good yield (75%). Following Johnson-type iodination,[70] Suzuki–Miyaura cross-coupling of the resulting 2-iodocyclopentenone **25** with boronate ester **24** proceeded smoothly at room temperature in the presence of silver(I) oxide[71] to give **30** in excellent yield. From here, we advanced **30** to the targeted macrocycle **23** by tandem Boc-thermolysis and acidic cleavage of the -TBS group (70% yield), followed by intramolecular Mitsunobu macrocyclization under dilute conditions, to give **23** in 80% yield.

Next, we turned our attention to functionalization of the cyclohexadiene portion of the macrocycle, targeting the vinyl epoxide originally envisioned at the outset of this campaign. All attempted electrophilic epoxidations (*m*-CPBA, DMDO, etc.) promoted rapid oxidation and aromatization, reviving an old challenge with these compounds. A slight modification to the macrocyclic scaffold was essential to overcoming this unwanted outcome: Weitz–Scheffer epoxidation[72] of the enone in **23** smoothly afforded epoxy-ketone **31** as a single diastereomer, which, upon treatment with a single equivalent of DMDO, successfully gave vinyl epoxide **32** in excellent yield.

We reasoned that, unlike enone **23**, epoxy-ketone **31** proved to be more resistant to spontaneous aerobic overoxidation due to the epoxide's inductive deactivation of the diene, thus facilitating productive reactivity with subsequent oxidation tactics. On the other hand, the electron-rich 2-position of the enone group in **23** might render the cyclohexadiene more oxidatively sensitive due to the increased hydridicity of the allylic C–H bonds. In support of this hypothesis, we reasoned that the observed site-selectivity for epoxidation of **31** might be explained by the relative electron-richness of the alkene at the 2-position of the cyclopentanone, rendering this position more reactive to DMDO-mediated epoxidation.

2.2.2. Transannular Reactivity of the Macrocyclic Intermediate. Installation of the vinyl epoxide in **32** enabled investigation of the macrocycle's transannular reactivity. In our initial design, we envisioned that upon cleavage of the –Ns group, the liberated amine would cyclize in an S_N' fashion to afford aza-bicyclo[3.3.1]nonane embedded within a 10-membered macrocycle. However, when the nosyl group in **32** was cleaved with PhSH and K_2CO_3, spontaneous transannular cyclization of the secondary amine occurred to give **33** as the sole isolated product (Figure 4A). In this system, transannular S_N cyclization at the tertiary allylic site of the epoxide (red position, Figure 4A) occurred preferentially over the desired S_N' cyclization (blue position, Figure 4A). In retrospect, we recognized that this selectivity might be due to the preorganization afforded by the macrocycle, perhaps driven by the conformational bias in **32** which places the methyl group in a pseudoequatorial orientation. Oxidation of alcohol **33** to the corresponding ketone (**34**) facilitated unambiguous structural characterization by X-ray crystallographic analysis, supporting our conformational analysis of the pseudoequatorially disposed methyl group.

Despite the structure observed in the crystalline solid-state, however, we observed broadened peaks in the solution phase ^{1}H NMR spectrum, indicating some degree of flexibility associated with tetracycle **34**. Although we expected transannular C–N bond formation to impart enhanced rigidity to the system, we reasoned that inversion of the tertiary amine might be responsible for the observed ^{1}H NMR signal broadening, either placing the alkyl chain in an axial (**34-*ax***) or pseudoequatorial (**34-*eq***) orientation (Figure 4B).

Addition of *d*-TFA confirmed our hypothesis: ^{1}H NMR of the resulting TFA ammonium salt displayed sharp peaks and revealed a 10:1 mixture of diastereomers, presumably about the now-static ammonium nitrogen center (Figure 4C). NOESY correlations identified **34-*ax*-TFA** as the major

https://doi.org/10.1021/jacs.4c11252
J. Am. Chem. Soc. 2024, 146, 33130–33148

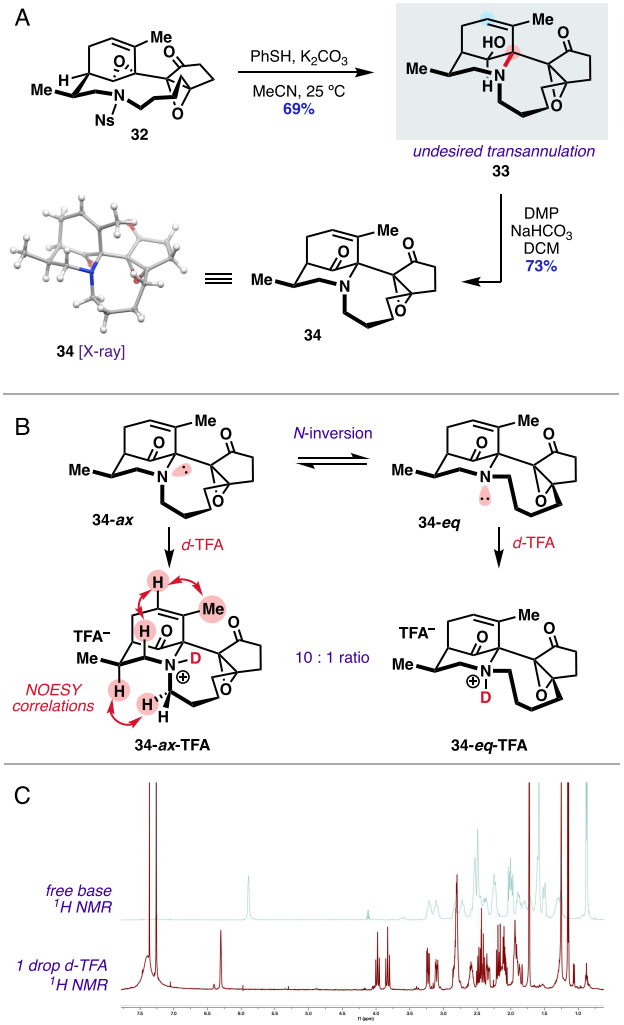

Figure 4. (A) Spontaneous transannulation observed upon −Ns cleavage. (B) Proposed equilibrium due to nitrogen inversion in **34** and identification of major diastereomer **34-*ax*-TFA** by addition of *d*-TFA. (C) ^{1}H NMR spectrum of **34** as the free base and *d*-TFA ammonium salt.

diastereomer (Figure 4B). While these ^{1}H NMR studies do not directly probe the originally proposed equilibrium between **34-*ax*** and **34-*eq*** (due to the possibility of a Curtin−Hammett scenario), this experiment suggested that some degree of flexibility about the tertiary amine is present in **34**.

From these conformational insights on **34**, we explored opportunities to carry out a 1,3-transposition to access our originally targeted aza-bicyclo[3.3.1]nonane (Scheme 3). In this approach, a suitable transition metal (such as Pd or Ni) could undergo oxidative addition to the allylic amine (or ammonium salt) to give π-allyl complex **35**. From here, rebound attack of the amine onto the electrophilic π-allyl species could give **36**, which we reasoned might be thermodynamically preferable due to formation of the conjugated enone moiety. Application of conditions from Yudin et al.[73] and Knowles et al.,[74] however, only returned the starting material. Attempts to enhance the leaving group ability of the amine by accessing enone **37** through Cp_2TiCl_2/Zn reduction did not provide an alternative solution to this stubborn isomerization problem. Other attempts to activate the amine by *N*-alkylation or *N*-oxidation were also unsuccessful, further confirming the steric challenge imposed

Scheme 3. Attempted 1,3-Transposition of the Amine by Generation of a π-Allyl Intermediate

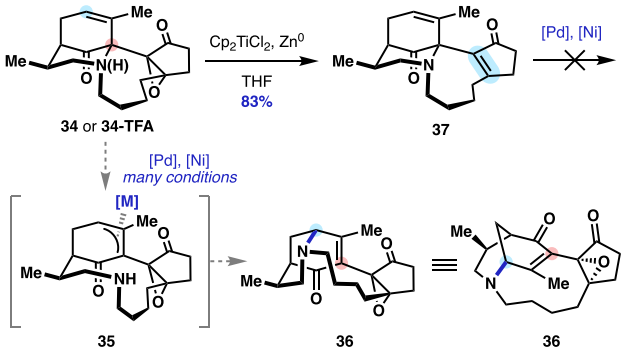

by aza-bicyclic intermediates of this type and suggesting that a post-transannulation isomerization might not be feasible.

2.2.3. Alternative Oxidation Strategies. Returning to macrocyclic diene **31**, we envisioned that a 1,4-oxidation pattern on the six-membered ring might complement the 1,2-oxidation strategy previously explored with vinyl epoxide **32**. Treatment of **31** with singlet oxygen generated bicyclic endoperoxide **39** and peroxyacetal **38** in 85% yield and 12% yield, respectively (Scheme 4A). While **39** presumably arises from [4 + 2] cycloaddition of singlet oxygen to diene **32**, a Schenk-ene pathway is likely responsible for the formation of **38**, which arises after acetalization of the resulting tertiary hydroperoxy group. Carrying endoperoxide **39** forward, we envisioned that a Kornblum−DeLaMare rearrangement[75] would establish the ketone at the southern position, leaving the northern hydroxy group available for transannular S_N amination. Upon treatment with DBU, however, hydroxy-enone **40** bearing the ketone at the undesired position was observed, likely due to the greater steric accessibility of the northern bridgehead proton in **39** for base-mediated elimination. Despite this setback, we aimed to form the desired aza-bicyclo[3.3.1]nonane by reductive amination. To that end, −Ns cleavage with PhSH and DBU afforded amine **41**, which appeared to exist in solution as the amino-enone instead of the cyclized hemiaminal. Unfortunately, all attempts to achieve a reductive amination were unsuccessful, either leading to decomposition or no observed reactivity.

Endoperoxide **39** presented additional opportunities for functional group manipulation in order to target our desired hydroxy-enone. Reduction of the O−O bridge with thiourea smoothly afforded *syn*-1,4-diol **42**, which, upon derivatization as the crystalline *bis*-ferrocene ester[76] (**45**, Scheme 4), enabled structural characterization by X-ray crystallographic analysis. Taking advantage of the inherent steric accessibility of the northern hydroxy group in **42**, treatment with one equivalent of acetic anhydride followed by addition of Dess−Martin periodinane gave **46** with the desired oxidation pattern.

With the targeted oxidation pattern in place, we sought to perform transannular S_N substitution between the amine and the acetylated hydroxy group in **46**. Cleavage of the acetyl group was carried out with K_2CO_3 in MeOH, affording hydroxy-enone **47** in 61% yield (Scheme 4). Upon −Ns cleavage with PhSH and DBU, however, immediate condensation of the resulting secondary amine onto the enone carbonyl was observed by ^{1}H NMR, as evidenced by the 1,1-disubstituted alkene formed in **48**.

https://doi.org/10.1021/jacs.4c11252
J. Am. Chem. Soc. 2024, 146, 33130−33148

Scheme 4. (A) Attempted Transannular Bond Formation from Intermediates Derived from Bicyclic Endoperoxide 39 and (B) [4 + 2] Cycloaddition Strategies Explored for the Functionalization of Diene 31

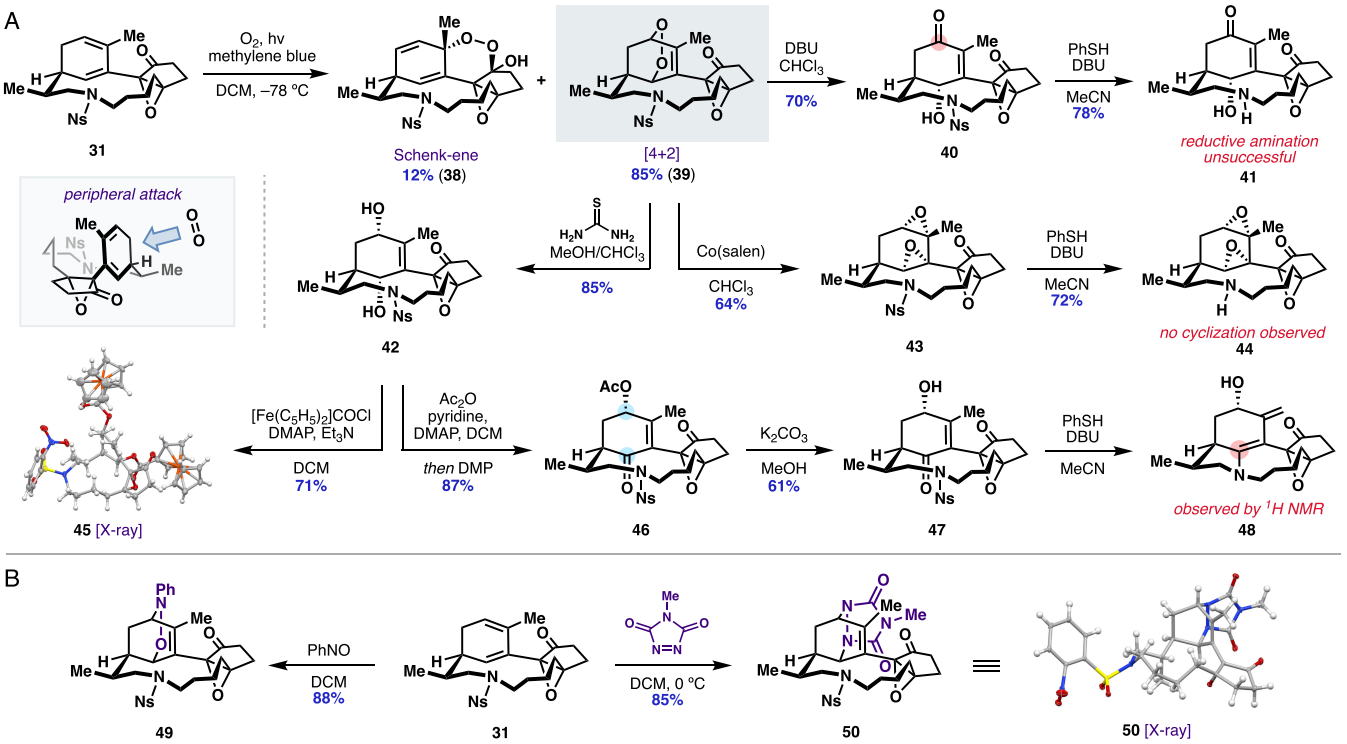

Endoperoxide **39** could also be isomerized by a Co-mediated rearrangement[77] to triepoxide **43** (Scheme 4), presenting an additional opportunity for transannulation analogous to vinyl epoxide **33**. Removal of the −Ns group with PhSH and DBU cleanly gave **44**; however, treatment of **44** with base surprisingly failed to promote any transannular epoxide opening, even at elevated temperatures. The structural subtleties between vinyl epoxide **33** and triepoxide **44** clearly led to vastly divergent reactivity, preventing the planned transannulation from taking place.

Despite the fact that we were unable to elaborate endoperoxide **39** to the intended transannulation product, we explored alternative hetero-[4 + 2] cycloadditions. Hoping to obtain improved chemoselectivity between substituents arranged in a 1,4-oxidation pattern, we found that treatment of **31** with nitrosobenzene afforded **49** in excellent yield as a single constitutional isomer and diastereomer, as confirmed by NOESY (Scheme 4B, see the Supporting Information for details). All attempts to reductively cleave the N−O bridge, however, led to either no reaction or nonspecific decomposition. On the other hand, we envisioned that derivatization of diene **39** with 4-methyl-1,2,4-triazoline-3,5-dione (MTAD)[78] might enable subsequent allylic substitution reactivity as recently demonstrated by Sarlah et al.[79] Exposure of **39** to MTAD at low temperatures smoothly led to **50**, which was unambiguously characterized by X-ray crystallographic analysis. Subsequent attempts to functionalize or displace the MTAD unit, however, were unsuccessful. At this stage, given the myriad strategies pursued to decorate the cyclohexadiene unit with the appropriate oxidation patterns required for transannulation, no further studies were conducted on this approach to **1**.

2.2.4. Conclusion of Our Approach to Himalensine A. At the outset of this synthetic campaign, we aimed to evaluate the hypothesis that retrosynthetic disconnections which maximally simplify a target's molecular graph (according to MolComplex) would result in maximally efficient total syntheses. In the case of himalensine A (**1**), this analysis identified an unusual transannular disconnection which suggested that macrocycles could serve as strategic intermediates for the construction of polycyclic skeletons such as the calyciphylline A-type core. However, several key factors complicated this molecular graph-inspired strategy. First, in this analysis, originally pioneered by Bertz,[10] structural complexity is taken as a direct proxy for synthetic complexity, suggesting that more structurally complex intermediates are inherently more challenging to synthesize and thus should be expressly minimized in the retrosynthetic disconnection. Macrocycle **11**, which was originally targeted for its structural simplicity relative to the target, proved to be synthetically inaccessible due to the instability shortcomings of intermediates **13** and **22**, which were prone to decomposition and overoxidation under the required reaction conditions. Despite their structural simplicity, macrocycles **11** and **23** displayed high synthetic complexity.

Second, this analysis overlooks the physical and conformational subtleties of the macrocyclic intermediate. Although macrocycles can display remarkable selectivity and unusual transannular reactivity due to the preorganization of key functional groups,[80−82] these properties can also thwart desired synthetic outcomes. In our case, the secondary amine in macrocycle **32** displayed a strong preference for engaging transannular functional groups at C8 rather than C4. We reason this is due to the conformational bias of the C18 methyl group, which is pseudoequatorially disposed, favoring the undesired outcome in this presumed Curtin−Hammett scenario.

https://doi.org/10.1021/jacs.4c11252
J. Am. Chem. Soc. 2024, 146, 33130−33148

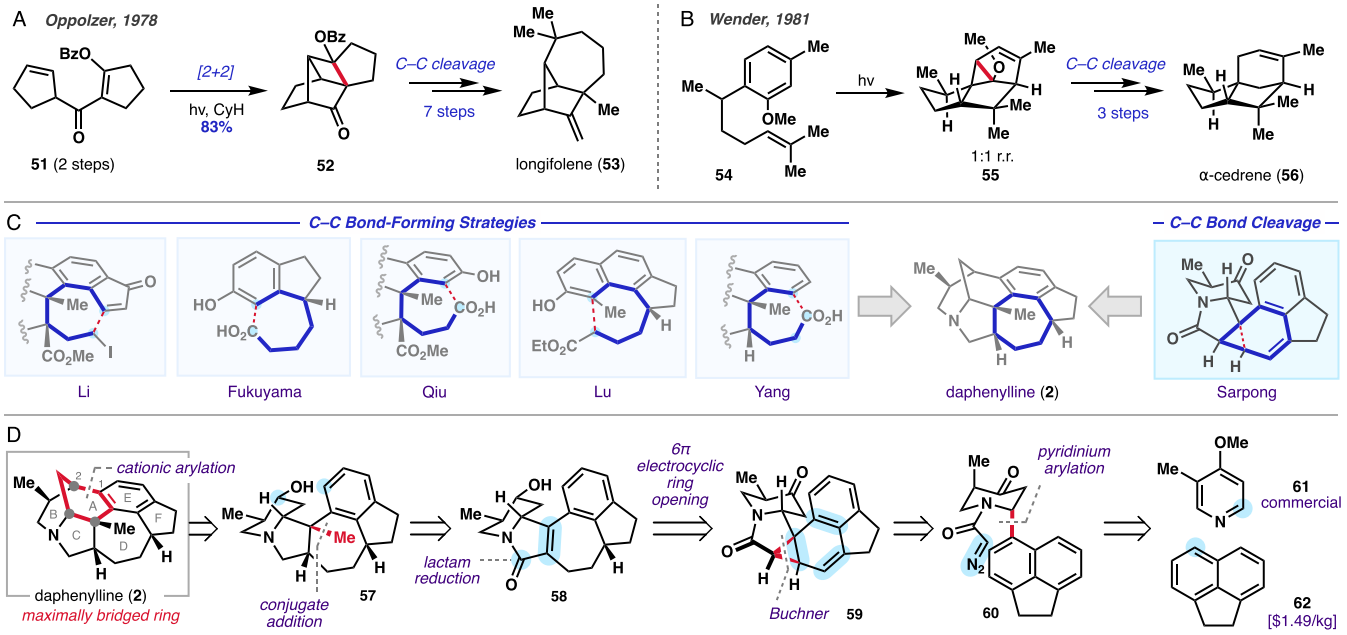

Figure 5. (A) Oppolzer's total synthesis of longifolene (**53**) using a [2 + 2]/C−C cleavage sequence. (B) Wender's synthesis of α-cedrene (**56**) using a meta-π-arene photocycloaddition and C−C cleavage. (C) Previous approaches to the seven-membered ring in the daphenylline (**2**) framework. (D) Retrosynthesis of daphenylline (**2**).

Finally, functional group compatibility was a challenging factor throughout the synthesis of macrocycles **11** and **23**. Preinstallation of the enone moiety, although attractive from the standpoint of minimizing redox manipulations, complicated the cyclohexadiene oxidation and required Weitz−Scheffer epoxidation to mask the cyclopentenone moiety. Cleavage of the −Ns group in hydroxy-enone **47** and vinyl epoxide **32** for instance, resulted in spontaneous unproductive transannular reactivity, precluding the possibility of reagent control in the site-selectivity challenges we faced. In view of these factors, we recognized that a purely molecular graph-based strategy, though intriguing as a case study for the application of computer-aided synthesis planning (CASP) tools, might be less successful than a hybrid approach which integrates several considerations.

2.3. Synthetic Strategy for Daphenylline. On the basis of the insights gained from our studies on himalensine A summarized above, we turned our attention to targeting another *Daphniphyllum* alkaloid, daphenylline (**2**) using a hybrid approach. Like himalensine A (**1**), daphenylline (**2**) shares much of the same calyciphylline A-type skeletal framework, including the hallmark aza-bicyclo[3.3.1]nonane core. However, **2** also contains an additional F-ring which, biosynthetically, is proposed to arise through Wagner−Meerwein-type shift of the canonical calyciphylline A-type core.[36,52] Since its isolation in 2009 from the fruits of *Daphniphyllum longeracemosum* by Hao and co-workers,[48] the structural complexity of daphenylline (**2**) has garnered significant attention from synthetic chemists, with eight total syntheses completed by Li et al.,[28,52] Fukuyama et al.,[30] Zhai et al.,[36] Qiu et al.,[83,84] Lu et al.,[40] Yang et al.,[41] and, recently, our own laboratory.[44] Given the notable synthetic advances on this scaffold previously reported by these other groups, we became similarly interested in using the complex molecular architecture of **2** as a platform for developing novel synthetic strategies to the *Daphniphyllum* alkaloids.

Here, we considered one of the primary assumptions made in the complexity analysis for **2**: that structural complexity can serve as a proxy for synthetic complexity. We recognized that there are notable exceptions to this principle. Routes which "overshoot" the target complexity of a synthetic target, such as Oppolzer's longifolene synthesis (**53**, Figure 5A) or Wender's synthesis of α-cedrene (**56**, Figure 5B), can be unexpectedly efficient. Indeed, these overly complex intermediates, termed "overbred intermediates" by Hoffmann,[85] can provide new avenues for preparing a targeted compound through subsequent bond cleavage tactics that are otherwise more challenging to synthesize by conventional strategies. In particular, cyclobutanes assembled by [2 + 2] photocycloaddition may be subject to a subsequent C−C bond cleavage to access the targeted carbon skeleton, as demonstrated by Baran et al.,[86] Luo et al.,[87] Dai et al.,[88] and others.[89]

In the context of the calyciphylline A-type *Daphniphyllum* alkaloids, we became inspired by this concept of "excess complexity" and the opportunity to showcase this underexplored strategy in a total synthesis of daphenylline (**2**). In our approach, we recognized that identification of the maximally bridged ring by network analysis might aid in simplification of the bridging AB-rings. According to network analysis of **2**, we determined that the benzo-fused A-ring is maximally bridged. Unlike previous approaches to the calyciphylline A-type scaffold (Figure 5C), we proposed that late-stage generation of the key aza-bicyclo[3.3.1]nonane core from an intermediate comprised entirely of fused rings would circumvent any challenges that might arise by carrying this complex structural motif forward through the rest of the synthesis. Furthermore, given C1−C2 bond formation in the forward sense might be aided by the inherent nucleophilicity of the pendant aromatic benzene ring, we proposed a retrosynthesis wherein daphenylline (**2**) might arise from pentacyclic piperidol **57** (Figure 5D). At that stage, we envisioned that **57** might be further simplified through removal of the quaternary methyl group, which, in the

https://doi.org/10.1021/jacs.4c11252
J. Am. Chem. Soc. 2024, 146, 33130−33148

forward sense, might arise through conjugate addition of a methyl nucleophile into α,β-unsaturated lactam **58** followed by lactam reduction.

We also recognized that the fused seven-membered ring, which had been previously constructed by others through radical[12,28,52,90] or Friedel−Crafts-type cyclization events[30,41,83] (Figure 5C), might arise through a C−C cleavage transformation from bicyclo[4.1.0]heptane **59**. In turn, norcaradiene **59** might arise through Buchner-type arene cyclopropanation of diazoacetamide **60**. This strategy has been previously demonstrated by Huisgen and Juppe,[91] Mander et al.,[92] and others[93,94] as a dearomative approach to seven-membered ring construction through a Buchner reaction/6π electrocyclic ring-opening sequence in the forward sense. Although this retrosynthetic "disconnection" counterintuitively *generates* a new C−C bond and *increases* structural complexity, access to the Buchner retron dramatically simplifies the construction of this motif, illustrating how "excess complexity" might, in certain cases, lead to more efficient synthetic outcomes.

Finally, we envisaged that diazoacetamide **60** might arise from dearomative pyridinium arylation of commercially available pyridine **61** and acenaphthene (**62**), which is an inexpensive byproduct of coal tar production. In this way, we planned our synthetic approach to daphenylline (**2**) from flat, aromatic starting materials **61** and **62** in which C−C bond formation and C−C bond cleavage would both play equally crucial and complementary roles in the overall sequence.

2.4. Development of a Total Synthesis of Daphenylline. *2.4.1. Synthesis of the Pentacyclic Core.* Our approach to daphenylline (**2**) began with a pyridinium dearomatization. Work from Comins and co-workers had established that treatment of 3-TIPS-4-methoxy-pyridine derivatives with a chloroformate, followed by addition of a Grignard reagent, afforded the 6-substituted dihydropyridone after hydrolytic workup. In this case, the bulky -TIPS substituent dictated the observed regioselectivity of the Grignard addition at the 6-position; methyl groups at the 3-position were known to give similar outcomes,[95] although the generality beyond TIPS-alkynyl lithiates was unknown. In our approach, we envisioned that dearomatizing arylation of commercially available **61** could give rise to the targeted arylated dihydropyridone. Treatment of **61** with Cbz-Cl, followed by Grignard reagent **63**, smoothly afforded 1,2-dihydropyridine **64** *in situ*, which gave dihydropyridone **65** in nearly quantitative yield after hydrolytic workup with aqueous HCl. Subjection of **65** to Comins' reduction conditions (Zn/AcOH),[96] followed by subsequent removal of the -Cbz group through hydrogenolysis with Pd/C in the same pot, gave the desired *anti*-disubstituted piperidone **66** in 91% yield. Diazoacetamide installation was achieved by adaptation of work from Fukuyama et al.[97,98] into a one-pot protocol: *N*-acetylation of **66** with bromoacetyl bromide, followed by S_N2 substitution with *bis*-Ts-hydrazide and TMG-mediated sulfinate elimination, gave diazoacetamide **60** in 76% yield (Scheme 5). This sequence was highly scalable, and decagram quantities of material could be easily carried through to **60**.

With facile access to diazoacetamide **60**, we extensively investigated the intramolecular Buchner cycloaddition (Figure 6A). Treatment with $Cu(hfac)_2$ at low temperatures gave norcaradiene **59** in moderate yield (40%, Figure 6B, entry 1). Careful analysis of the isolated side products revealed that homodimer **67** was isolated in 15% yield. Acceptor carbenes

Scheme 5. Preparation of Diazoacetamide 60 from Aromatic Starting Materials 61 and 63

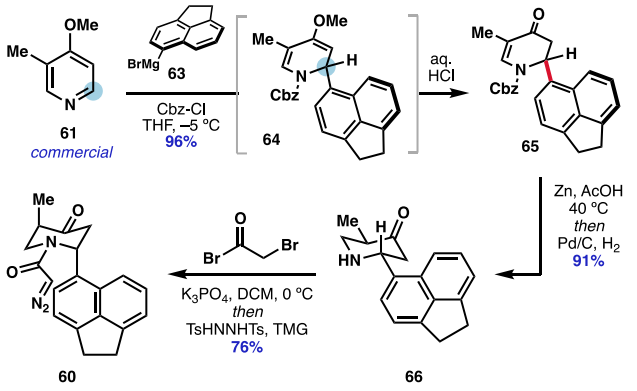

are known to undergo homodimerization as a common side reaction, especially when intramolecular Buchner cyclopropanation is slow.[99] Slow addition of **60** over 15 min suppressed formation of **67** (entry 2). A brief survey of temperatures and concentrations (entries 3−6) with this catalyst was unfruitful, and no clear trends were observed. Screening Rh-based catalysts highlighted the formation of an additional side product, **68**, likely the result of insertion into adventitious water in the reaction mixture (entries 8−11). The use of 4 Å molecular sieves, along with slow addition of **60** by syringe pump over 4 h (entries 12 and 13), minimized the formation of **67** and **68** with $Rh_2(OAc)_4$ emerging as the best-performing catalyst (55% yield, entry 14).

With optimal conditions identified for Buchner cycloaddition, we began exploring strategies to promote cleavage of the endocyclic C−C bond in vinyl cyclopropane **59**, which we structurally characterized by X-ray crystallographic analysis (Figure 6A). With the intent of generating a cyclopropylcarbinyl radical through halogen abstraction, treatment of **59** with NBS in the presence of water effected a bromo-hydration of the trisubstituted alkene, giving crystalline bromohydrin **69** in a modest 33% yield (Figure 6C). Unfortunately, all attempts to cleanly fragment the endocyclic C−C bond with Bu_6Sn_2 or Ag(I) salts were met with failure, either promoting decomposition or returning unreacted starting material.

Additional strategies were also pursued: Rh(III)-arene complexation,[100] intended to lower the aromatic stabilization energy of the benzene ring in **59** and promote 6π electrocyclic ring opening, gave no discernible product. Exposure to arenophiles such as MTAD[101] failed to give any [4 + 2] cycloaddition reactivity; attempted Birch reduction was similarly unfruitful. Finally, irradiation of **59** with triplet sensitizers or with a medium-pressure Hg lamp did not lead to any cyclopropane fragmentation through an intended triplet biradical intermediate.

Given the challenges faced in identifying a set of mild conditions for endocyclic C−C bond cleavage, we turned to the previously explored thermal 6π-electrocyclic ring opening. Heating a dilute solution (0.05 M) of **59** in 1,2-dichlorobenzene in a microwave reactor at 200 °C for 45 min gave partial conversion to desired cycloheptadiene **71** along with an unexpected side product, which we have tentatively assigned by ^{1}H/COSY NMR as cycloheptadiene **72** (Table 1, entry 1). We postulate that, mechanistically, disrotatatory 6π electrocyclic ring opening gives rise to dearomatized intermediate **70**, which then undergoes facile

https://doi.org/10.1021/jacs.4c11252
J. Am. Chem. Soc. 2024, 146, 33130−33148

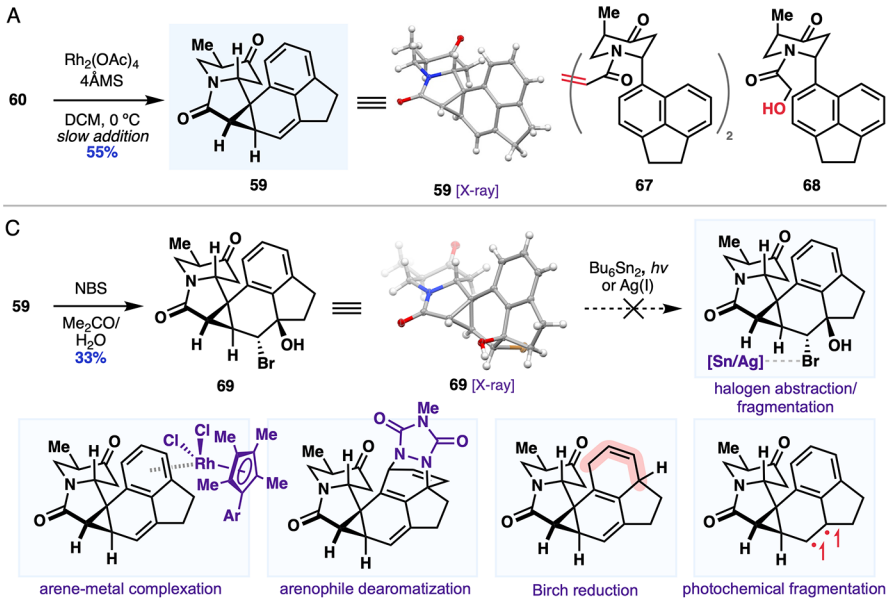

B

entry	conditions	method	result[a]
1	$Cu(hfac)_2$, 0 °C	A	**59**: 40%, **67**: 15%
2	$Cu(hfac)_2$, 0 °C	B	**67**: < 15%
3	$Cu(hfac)_2$, –40 °C to rt	B	**59**: 44%
4	$Cu(hfac)_2$, –78 °C to rt	B	**59**: 35%
5	$Cu(hfac)_2$, 0.1 M, 0 °C	A	**59**: 29%
6	$Cu(hfac)_2$, 0.01 M, 0 °C	B	**59**: 31%
7	$Cu(hfac)_2$, 0 °C, air	B	**59**: 32%
8	$Rh_2(OAc)_4$, 0 °C	B	**59**: 55%, **68**: 22%
9	$Rh_2(TCPTTL)_4$, 0 °C	B	**59**: 33%, **68**: 13%
10	$Rh_2(S\text{-}PTTL)_4$, 0 °C	B	**59**: 10%, **68**: 22%
11	$Rh_2(OAc)_4$, 0 °C, azeo.	B	**59**: 54%, **68**: 21%
12	$Cu(hfac)_2$, 4Å MS, 0 °C	C	**59**: 45%, unk: 22%
13	$Rh_2(esp)_2$, 4Å MS, 0 °C	C	**59**: 46%, **67**: 36%
14	$Rh_2(OAc)_4$, 4Å MS, 0 °C	C	**59**: 55%[b], **67**: < 5%

Procedure A: addition of catalyst to **60**
Procedure B: 15 min addition of **60** to catalyst
Procedure C: 4 h addition of **60** to catalyst

Figure 6. (A) Intramolecular Buchner cycloaddition to access norcaradiene **59** and side products **67** and **68**. (B) Table of conditions screened for Buchner reaction. (C) Initial attempts to cleave the endocyclic C−C bond through radical fragmentation or dearomatization tactics. [a]Yields determined by ^{1}H NMR relative to pyrazine as an internal standard.

Table 1. Optimization of 6π-Electrocyclic Ring-Opening Cascade[a]

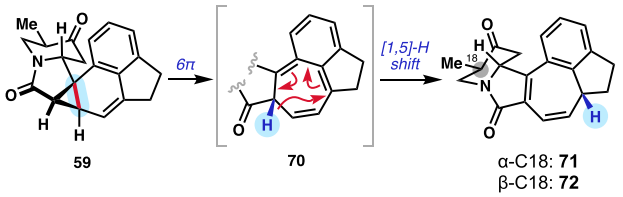

entry	time (min)	temp. (°C)	conc. (M)	59:71:72	yield (71)
1	45	200	0.05	1:0.69:0.64	27%
2	45	230	0.05	0.21:1:0.42	46%
3	15	230	0.025	0.18:1:0.36	44%
4	5	250	0.0.5	0.18:1:0.26	52%
5	5	260	0.025	0:1:0.37	20%
6	5	250	0.025	0:1:0.05	79%

[a]Product ratios determined by ^{1}H NMR.

suprafacial [1,5]-hydride shift to restore aromaticity and afford the key methine stereocenter in **71**. However, observation of **72** also pointed to the possibility of methyl epimerization from **71**, complicating the optimization of this transformation for obtaining the desired cycloheptadiene without undesired autoenolization and epimerization at these elevated temperatures. Reasoning that if **71** is an intermediate en route to **72**, shorter reaction times might improve the isomer ratio, heating **59** for 15 min at 230 °C gave improved conversion and yields of **71** (entry 2). In an attempt to promote unimolecular reactivity over unwanted decomposition pathways, we tried further dilution of the reaction mixture to 0.025 M, but a similar yield was obtained (entry 3). Heating for 5 min at 250 °C further improved the reaction outcome (entry 4), although temperatures beyond 250 °C proved deleterious to the yield and isomer ratio (entry 5). Finally, we identified that short reaction times (5 min) at 250 °C using highly dilute concentrations (0.025 M) gave essentially quantitative conversion to **71** with minimal isomer formation, affording **71** in 79% yield after chromatographic purification due to slight instability on silica gel (entry 6).

With optimal conditions for producing **71** in hand, we began to investigate our planned sequence for alkene hydrogenation and methyl conjugate addition. Treatment of **71** with hydrogen and Pd/C smoothly gave **73** in 83% yield, which allowed us to unambiguously assign the connectivity by X-ray crystallography (Scheme 6A). At this stage, we envisioned that 1,4-addition of a methyl nucleophile would establish the requisite quaternary methyl stereocenter. However, treatment of **73** with methyl cuprate (Gilman's reagent) resulted in competitive 1,2-addition into the ketone group, giving **74**. Similarly, with the intent of installing the quaternary methyl group by a cyclopropanation/hydrogenolysis sequence, subjection of **73** to Corey−Chaykovsky cyclopropanation gave epoxide **75** instead. Many additional conjugate addition conditions were also surveyed, either resulting in competitive ketone 1,2-addition or no observed reactivity.

Given the chemoselectivity challenges we faced with competing addition to the ketone group in the attempted conjugate addition to unsaturated lactam **73**, we sought to reduce the ketone to the corresponding alcohol. The ketone group in **73** was easily reduced with $NaBH_4$ to give alcohol **58** in 93% yield. However, subjection of **58** to a broad range of methyl addition strategies failed to produce the desired *β*-methylation product, either returning starting material or isomers of **76**. We attribute this reactivity to 1) the crowded steric environment of the tetrasubstituted alkene and 2) deprotonation or tautomerization of the C4 position to give deactivated 2-hydroxypyrroles (such as **76**), as evidenced by observed epimerization at this position. This tautomerization to **76** would not only shut down the electrophilic reactivity of the unsaturated lactam, but also ablate a stereocenter on the piperidine unit. Radical methylation, using conditions from Doyle and co-workers,[102] gave nonspecific decomposition, likely attributable to the propensity of methyl radical to undergo HAT processes with substrates possessing many weak C−H bonds.

https://doi.org/10.1021/jacs.4c11252
J. Am. Chem. Soc. 2024, 146, 33130−33148

Scheme 6. (A) Attempted Installation of the Methyl Group by Conjugate Addition into Unsaturated Lactam 73 and (B) Unsuccessful Diene Functionalization Strategies to Aid Methyl Group Installation

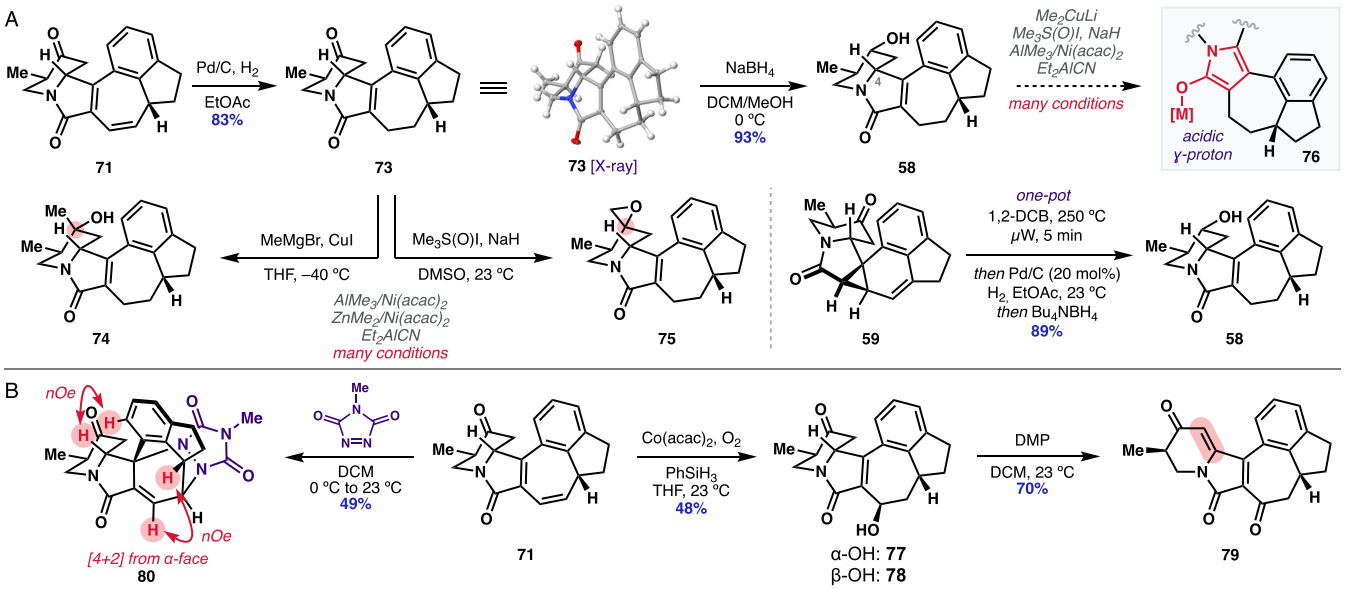

Scheme 7. (A) Revised Methyl Installation Based on Photochemical C−C Bond Generation and Single-Atom Excision, (B) Prefunctionalized Cyclobutanes Prepared by [2 + 2] Photocycloaddition, and (C) Mechanistic Hypothesis for Observed Head-to-Tail Selectivity

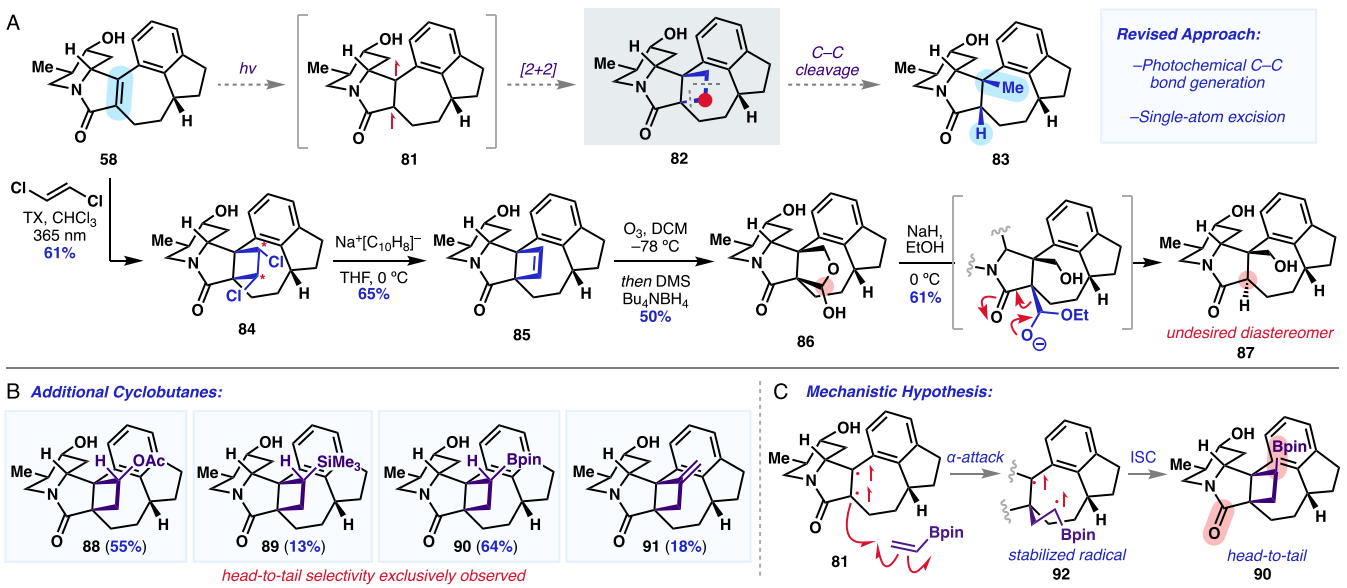

Concurrently, we also developed streamlined conditions that enabled us to telescope the 6π-electrocyclic ring opening with the hydrogenation/ketone reduction sequence in a single step (Scheme 6A). In this way, **59** could be heated in a microwave reactor to give **71** *in situ*, after which hydrogenation with Pd/C and addition of a soluble hydride source (Bu_4NBH_4) smoothly afforded **58** in a one-pot, one-step procedure (89% yield).

At this juncture, we recognized the challenges associated with nucleophilic addition into **73** or **58** given the weakly electrophilic nature of the α,β-unsaturated lactam. Instead, we envisioned that functionalization of diene **71** might present opportunities for subsequent installation of the methyl group. To that end, Mukaiyama hydration of **71** gave **77** and **78** as a 1:1 mixture of diastereomers (Scheme 6B). Hoping to arrive at the corresponding enone, which might display greater electrophilicity toward conjugate methylation, we treated **77** with Dess−Martin periodinane; instead, overoxidation to pyridone **79** was observed. A short survey of milder DMSO-based oxidation conditions indicated that this overoxidation might be spontaneous in the presence of air.

Additional studies were performed to engage the diene in a [4 + 2] cycloaddition to alter the diminished reactivity of the unsaturated lactam. Exposure of **71** to singlet oxygen returned only starting material. Use of a highly electrophilic dienophile, such as MTAD, led to the formation of **80** in modest yield through [4 + 2] cycloaddition on the α-face of the diene. The diastereoselectivity of this transformation was surprising and raised questions about the proposed facial selectivity for installation of the methyl group if dienophiles such as MTAD preferentially approached from the α-face. Further attempts to

https://doi.org/10.1021/jacs.4c11252
J. Am. Chem. Soc. 2024, 146, 33130−33148

open the MTAD adduct through oxidative addition using $Pd(PPh_3)_4$,[79] however, led to no discernible product.

Taken together, we had exhaustively investigated the methyl group installation by nucleophilic addition, radical Giese addition, intramolecular pericyclic reactivity, and transition metal π-allyl substitution. In our hands, all attempts had failed, either due to the tempered electrophilicity of the unsaturated lactam or undesirable side-reactivity of other present functional groups.

2.4.2. [2 + 2] Photocycloaddition Approach. At this stage, given our repeated failed attempts to methylate through nucleophilic addition, we envisioned that generation of triplet biradical **81** from **58** could enable productive C−C bond construction through [2 + 2] cycloaddition. However, formation of a four-membered ring would then present a new challenge, wherein subsequent single-atom excision from **82** would be required to yield the formal *syn*-hydromethylation product (**83**, Scheme 7A).

Initial efforts toward this goal began with unsaturated lactam **58**, which we envisioned would only have one chromophore for triplet excitation. Irradiation of **58** in the presence of 1,2-dichloroethylene and thioxanthone gave cyclobutane **84** as a mixture of diastereomers, our first success in forming the long-desired C−C bond (Scheme 7A). Subsequent dissolving metal reduction with sodium naphthalenide cleanly afforded cyclobutene **85**, an unusually strained [5.3.2]propellane. From here, we envisioned that oxidative cleavage might execute the planned sequence illustrated in Scheme 6A. To that end, ozonolysis of **85** at low temperature, followed by addition of Me_2S to the putative dialdehyde intermediate, yielded a mixture that decomposed on silica gel and was sensitive to protic solvents. However, quenching the proposed dialdehyde intermediate with Bu_4NBH_4 afforded lactol **86** as a single isomer, with exclusive reduction of the distal aldehyde, the resulting alcohol of which concomitantly cyclized into the proximal aldehyde. Next, we envisioned that lactol opening and retro-Claisen condensation would provide our desired intermediate. However, although treatment of **86** with NaH and EtOH successfully excised the more oxidized carbon, undesired diastereomer **87** was exclusively formed under the (presumably thermodynamically controlled) reaction conditions.

In an effort to carry out C−C cleavage in a catalyst-controlled, stereospecific fashion, we targeted cyclobutanes that contained the necessary functional handles for this reactivity. Under similar reaction conditions as above, [2 + 2] photocycloaddition was performed with vinyl acetate, vinyl trimethylsilane, vinyl pinacol boronate, and allene, leading to **88**−**91**, respectively (Scheme 7B). Despite our success in accessing these intermediates, however, exclusive head-to-tail selectivity was observed in each of these cases, preventing us from performing C−C cleavage which might be accelerated by the neighboring lactam carbonyl. Given the observed head-to-tail selectivity, we postulated that stepwise [2 + 2] cycloaddition might occur by initial attack of the α-radical in **81** (Scheme 7C) onto the alkene to give **92**, placing the radical at the more stabilized position. Following intersystem crossing, radical recombination to **90** would occur.

Despite the setbacks we experienced with the all-carbon [2 + 2] photocycloadditions, we became intrigued by the possibility that a Paternò−Büchi reaction might offer new possibilities, especially at the bond cleavage stage of the sequence. Padwa employed thioamides in an intramolecular thia-Paternò−Büchi strategy to form C−C bonds via thietane intermediates, which were desulfurized with Raney nickel in a subsequent step.[103] In terms of the head-to-tail selectivity, we were encouraged by the fact that alkyllithium reagents are known to react with thiones at sulfur instead of carbon, perhaps due to the stabilized α-thio-anion. Recently, Liu and co-workers reported a mild Ir(III)-photosensitized intermolecular thia-Paternò−Büchi reaction with xanthates and trithiocarbonates to generate a range of thietanes.[104]

In view of these insights, we investigated a thia-Paternò−Büchi photocycloaddition. Irradiation of **58** with 400 nm blue LED in the presence of $Ir(dF(CF_3)ppy)_2dtbbpy]PF_6$ and excess methyl trithiocarbonate (**93**) afforded small quantities of thietane **94** with the desired head-to-head selectivity, as evidenced by NOESY NMR experiments (entry 1, Figure 7A).

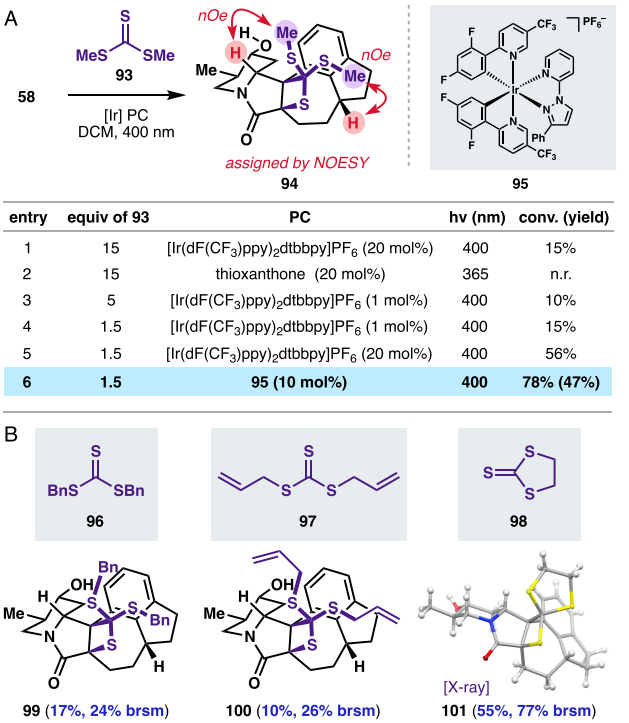

entry	equiv of 93	PC	hv (nm)	conv. (yield)
1	15	$[Ir(dF(CF_3)ppy)_2dtbbpy]PF_6$ (20 mol%)	400	15%
2	15	thioxanthone (20 mol%)	365	n.r.
3	5	$[Ir(dF(CF_3)ppy)_2dtbbpy]PF_6$ (1 mol%)	400	10%
4	1.5	$[Ir(dF(CF_3)ppy)_2dtbbpy]PF_6$ (1 mol%)	400	15%
5	1.5	$[Ir(dF(CF_3)ppy)_2dtbbpy]PF_6$ (20 mol%)	400	56%
6	**1.5**	**95 (10 mol%)**	**400**	**78% (47%)**

Figure 7. (A) Optimization table for thia-Paternò−Büchi [2 + 2] photocycloaddition. (B) Additional thietanes prepared by [2 + 2] photocycloaddition.

Following this initial result, we investigated the optimization of this transformation to improve the yield of **94.** The use of stronger triplet sensitizers and more energetic UV light failed to give any product (entry 2). Despite the large excess of **93**, we were puzzled at the low conversion to **94**, even after extended reaction times (18 h). Noting that Liu and co-workers suggest from Stern−Volmer quenching studies that species analogous to **93** are competent triplet quenchers, we postulated that excess **93** might prevent the necessary triplet excitation of **58** from the Ir(III)* species by premature triplet quenching. Lowering the equivalents of **93** and Ir(III) catalyst led to similar degrees of conversion (entries 3−4). Finally, we found that conditions similar to those employed by Liu and co-workers involving 1.5 equiv of **93** and 20 mol % of Ir(III) photocatalyst gave an improved 56% conversion (entry 5), which was further boosted to 78% conversion and 47% isolated yield with only 10 mol % loading of catalyst **95** (entry 6),

https://doi.org/10.1021/jacs.4c11252
J. Am. Chem. Soc. 2024, 146, 33130−33148

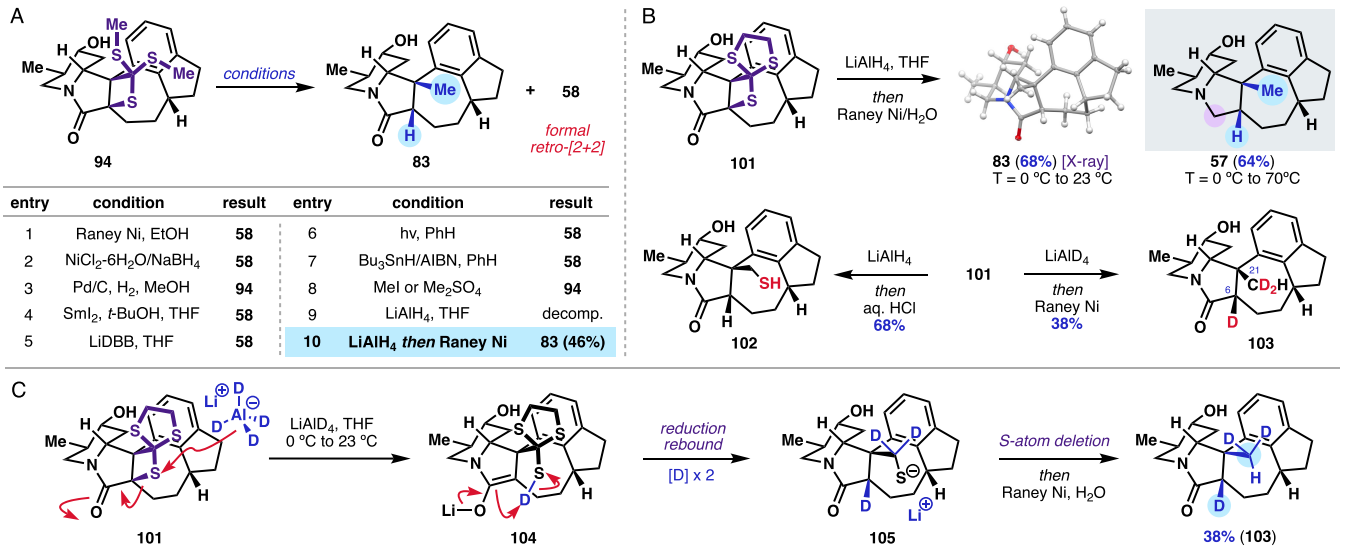

entry	condition	result	entry	condition	result
1	Raney Ni, EtOH	58	6	hv, PhH	58
2	$NiCl_2$-$6H_2O$/$NaBH_4$	58	7	Bu_3SnH/AIBN, PhH	58
3	Pd/C, H_2, MeOH	94	8	MeI or Me_2SO_4	94
4	SmI_2, *t*-BuOH, THF	58	9	$LiAlH_4$, THF	decomp.
5	LiDBB, THF	58	**10**	**$LiAlH_4$ *then* Raney Ni**	**83 (46%)**

Figure 8. (A) Attempted reduction of thietane **94**. (B) Formal *syn*-hydromethylation by $LiAlH_4$/Raney Ni reduction of thietane **101** and initial mechanistic experiments. (C) Proposed mechanism for thietane reduction and desulfurization.

which is reported to have a high triplet energy (62.1 kcal/mol) and exceptionally long triplet lifetime (2.230 μs).[104]

With these conditions identified for the thia-Paternò–Büchi reaction with **93** (entry 6, Figure 7A), we explored additional trithiocarbonates suitable for this transformation (Figure 7B). Benzyl trithiocarbonate (**96**) and allyl trithiocarbonate (**97**) gave rise to the corresponding thietanes, **99** and **100**, respectively, albeit in low yields. The use of trithiocarbonate **98** yielded spirocyclic thietane **101** in an improved 55% yield (77% brsm). This allowed us to unambiguously confirm the structure of **101** by X-ray crystallographic analysis.

Having prepared a series of thietanes, we set out to perform the desulfurization step of the planned sequence. Treatment of **94** or **101** with Raney nickel, however, led to the unexpected recovery of unsaturated lactam **58** (Figure 7A, entry 1). Though surprising, the formal retro-[2 + 2] might occur through β-scission or β-elimination processes upon oxidative addition of Ni^0. Although the exact mechanism of Raney nickel desulfurization is not well understood, biradical intermediates have been invoked in a number of contexts,[105] and we reasoned that a 1,4-biradical formed upon rupture of the strained thietane might rapidly fragment to return the trithiocarbonate and lactam **58**.

We next began an extensive campaign to explore reduction strategies of the thietane to the desired methylated intermediate (Figure 7A). First, treatment with other nickel hydride sources (such as $NiCl_2$/$NaBH_4$, entry 2) gave similar retro-[2 + 2] fragmentation outcomes. Milder hydrogenation catalysts, such as Pd/C (entry 3), gave no reaction, however. Single-electron reductants such as SmI_2 (entry 4) or LiDBB[106] (entry 5) gave complex mixtures with **58** as the major product. Interestingly, direct irradiation with a medium-pressure Hg lamp (entry 6) also promoted fragmentation to **58**, raising the possibility that the thia-Paternò–Büchi is reversible under the blue LED/triplet sensitization conditions. Reduction with Bu_3SnH/AIBN (entry 7) at elevated temperatures also cleanly gave **58**, suggesting that any radical-based fragmentation is likely to lead to facile β-scission back to **58**. In an attempt to form a sulfonium ylide, which might undergo retro-ene fragmentation, **94** was treated with MeI or Me_2SO_4, but no reaction was observed (entry 8).

On the basis of these insights involving the reactivity of **94** with metal hydrides, single-electron reductants, and radical-generating reagents, we turned our attention to more potent hydride sources. Treatment of **94** with $LiAlH_4$ led to immediate formation of a new intermediate, which proved challenging to isolate using the standard Fieser–Fieser workup.[107] However, LCMS analysis of the crude mixture indicated the presence of sulfur-containing intermediates which might require desulfurization prior to isolation. As a result, we repeated the reduction of **94** with $LiAlH_4$, now quenching with a Raney Ni/H_2O slurry, which successfully gave β-methylated lactam **83** in a modest 46% yield (entry 10). Subjecting spirocyclic thietane **101** to the same conditions yielded **83** in an improved 68% yield, enabling unambiguous structural confirmation of this result by X-ray crystallographic analysis (Figure 8B). Performing the reduction at elevated temperatures (70 °C) conveniently allowed for concomitant reduction of the lactam, affording methylated pyrrolidine **57** in similar yields (64%).

We next studied the reduction mechanism of thietane **101** in greater detail. Quenching the reaction with HCl in the absence of Raney Ni afforded thiol **102**, suggesting that this thiol is an intermediate prior to desulfurization. Isotopic labeling studies with $LiAlD_4$ and Raney Ni yielded trideuterated compound **103**, with D-incorporation observed twice on the C21 methyl and once at C6. This result suggested that $LiAlH_4$, rather than Raney Ni, is responsible for the *syn*-stereochemistry at C6. With these insights, we propose a mechanism wherein $LiAlD_4$ attacks the thietane sulfur atom in **101** to afford enolate **104**, which is then kinetically quenched by the pendant thiol in a "reduction-rebound" mechanistic sequence (Figure 8C). After further reduction of the thio-orthoformate to intermediate thiol **105**, final Raney Ni-mediated desulfurization affords **103** with water or solvent as the presumed proton or hydrogen atom source.

2.4.3. Completion of the Total Synthesis. Now that the thia-Paternò–Büchi had enabled the installation of the long-sought quaternary methyl group, we aimed to achieve formation of the final C–C bond to access daphenylline (**2**). We envisioned that a Grewe cyclization, wherein a highly electrophilic dication formed from ionization of the hydroxy

https://doi.org/10.1021/jacs.4c11252
J. Am. Chem. Soc. 2024, 146, 33130–33148

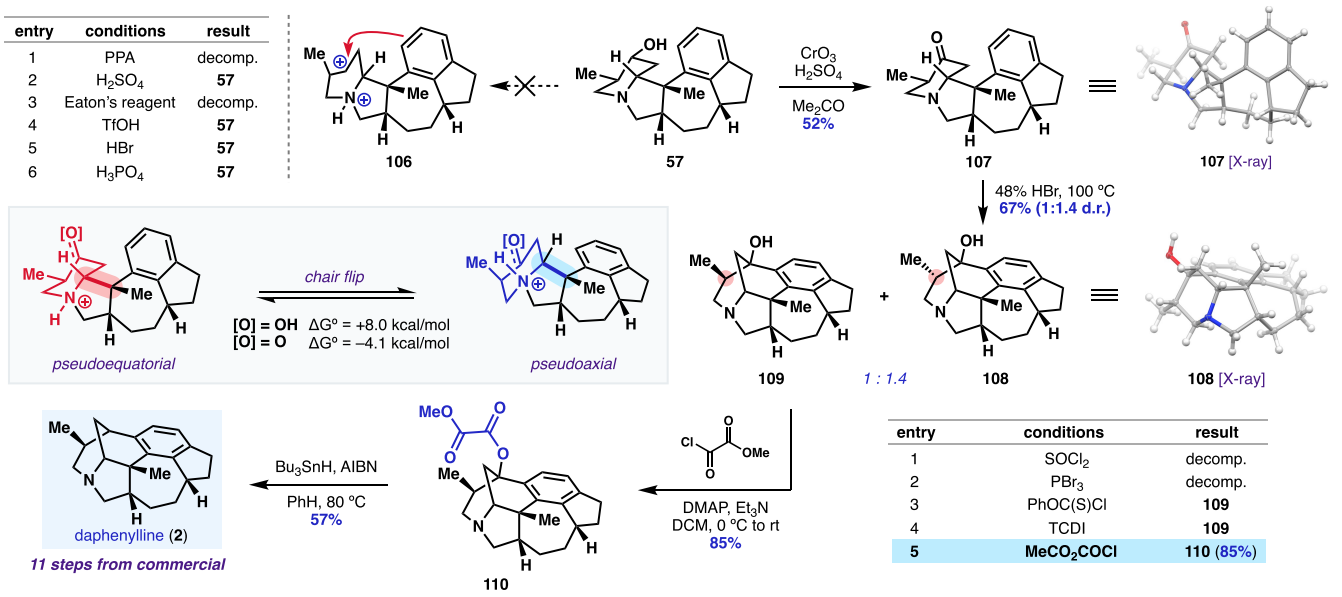

Figure 9. Completion of the total synthesis of daphenylline (**2**) by final Friedel−Crafts-type cyclization and bridgehead deoxygenation. All calculations were performed with Gaussian 15 rev. C.01 at the M06-2X/def2-TZVP//M06-2X/def2-SVP level of theory. See the Supporting Information for full computational details and references.

group on the ammonium species, would provide direct access to daphenylline (**2**) through capture of the secondary carbocation from the nearby arene (Figure 9).[108] To this end, we surveyed a series of strong Brønsted acids to promote this dication formation, including polyphosphoric acid, Eaton's reagent,[109] triflic acid, and HBr, all of which had been previously used in this kind of transformation. Unfortunately, all attempted Grewe cyclizations resulted either in nonspecific decomposition or returned **57**. We wondered whether the required pseudoequatorial or chair-flipped conformation of **57** would be challenging to access, even at elevated temperatures. Furthermore, we recognized that the putative dication species (**106**) might undergo undesirable carbocation rearrangements which would prevent the desired cyclization from occurring.

With these insights in mind, we imagined that the corresponding ketone might offer analogous possibilities in a Friedel−Crafts-type cyclization, which, after subsequent deoxygenation might finally afford daphenylline (**2**). Oxidation of **57** proceeded in modest yield to give ketone **107**; a short screen of conditions identified Jones oxidation conditions to give highest yields (52%), which enabled unambiguous structural assignment by X-ray crystallographic analysis (Figure 9). Treatment of **107** with 47% HBr at elevated temperatures (100 °C) successfully gave the desired aza-bicyclo[3.3.1]-nonane **109** along with **108** as a 1:1.4 mixture of diastereomers about the secondary methyl group in a combined 67% yield. This observed mixture of diastereomers is likely due to acid-promoted enolization and epimerization of ketone **107** prior to productive C−C bond formation. The minor diastereomer (**108**) was characterized by X-ray crystallographic analysis, confirming the connectivity of this milestone bridged bicyclic intermediate.

To further probe the observed difference in reactivity between piperidol **57** and piperidone **107** with respect to the desired cyclization, conformational equilibria between pseudoequatorial and pseudoaxial chair conformations of **57** and **107** were further investigated with density functional theory calculations at the M06-2X/def2-TZVP//M06-2X/def2-SVP level of theory (Figure 9). In their neutral forms, both compounds strongly favor the pseudoequatorial conformation by more than 10 kcal/mol^{-1} (see the Supporting Information for full details). Following tertiary amine protonation, the difference in conformer stability is reduced by several kcal mol^{-1}, although the pseudoequatorial form is still more favorable. Upon protonation of the carbonyl oxygen in **107**, the chair flip to form the pseudoaxial conformer becomes exergonic with ΔG = −4.1 kcal mol^{-1}, whereas for alcohol **57** this remains endergonic (ΔG = +8.0 kcal mol^{-1}). Since accessing the pseudoaxial conformer is necessary for C−C bond formation, these observations are consistent with the reactivity of **107** toward cyclization as compared to **57**. Stabilization of the pseudoaxial conformer occurs when the oxocarbenium ion is in close proximity to an aromatic C−H bond (2.24 Å): Natural Bonding Orbital (NBO) analysis suggests a favorable donor−acceptor interaction between these groups worth 6.1 kcal mol^{-1} (see Figure S14 in the Supporting Information).

With the azabicycle constructed, we turned our attention to removal of the bridgehead hydroxy group to arrive at daphenylline (**2**). Initial attempts to convert the bridgehead hydroxy group into an easily reducible chloride, bromide, or xanthate were met with resistance, leading either to recovered starting material or nonspecific decomposition. Activation of the bridgehead alcohol group with methyl oxalyl chloride,[110] however, successfully gave **110** in good yield (85%) after purification by a short silica plug. From here, Barton−McCombie deoxygenation with Bu_3SnH/AIBN produced daphenylline (**2**) in 57% yield, completing the total synthesis of this complex *Daphniphyllum* alkaloid target. All spectral data for **2** were found to be in agreement with both natural and synthetically prepared material reported in the literature. Taken together, daphenylline was synthesized from commercially available material in a total of 11 steps in racemic form, representing the shortest total synthesis reported to date.

Having completed the racemic total synthesis of daphenylline (**2**), we next sought to achieve an enantioselective

https://doi.org/10.1021/jacs.4c11252
J. Am. Chem. Soc. 2024, 146, 33130−33148

synthesis of (−)-**2**. We recognized that piperidone intermediates such as **66** might be prepared by enantioselective conjugate addition of an aryl nucleophile into a dihydropyridone. Hayashi and co-workers[111] reported this transformation with Rh complexes using (*R*)-BINAP as the ligand, enabling 1,4-addition of arylzinc reagents into Cbz-protected dihydropyridone **111**, affording enantioenriched pyridones in high yield and enantioselectivities (Figure 10). Replication of these conditions with acenaphthene-derived arylzinc **112**, however, gave only modest yields of **113** and poor enantioselectivities.

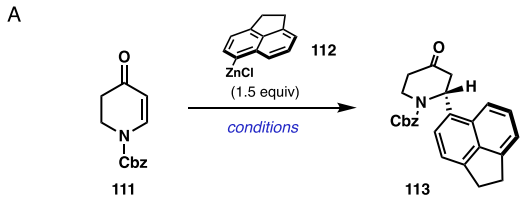

entry	method	ligand	yield	*ee*
1	A	(*R*)-BINAP	10%	49%
2	A	(*R*)-SEGPHOS	< 5%	60%
3	A	Josiphos SL009	66%	< 5%
4	A	(*S*,*S*)-DPP-pentane	29%	−79%
5	A	(*R*,*R*)-Ph-BPE	17%	−98%
6	B	(*S*,*S*)-Ph-BPE	44%	98%
7	C	(*S*,*S*)-Ph-BPE	60%	99%

A: $[Rh(C_2H_4)Cl]_2$ (5 mol%), L (11 mol%), ArZnCl (1.5 equiv)
B: ArZnCl from $ArMgBr/ZnCl_2$ (heterogeneous)
C: ArZnCl from $ArMgBr$-$LiCl/ZnCl_2$ (homogeneous)

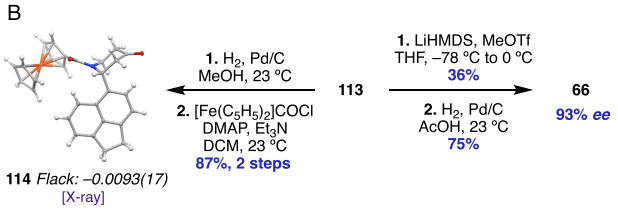

Figure 10. (A) Optimization of enantioselective Rh-mediated conjugate addition of arylzinc **112** into dihydropyridone **111**. (B) Confirmation of the absolute configuration of **113** and conversion to enantioenriched piperidone **66**.

Despite the challenges faced with the initial Hayashi conditions, we began a thorough optimization of this transformation (Figure 10A). For the sake of convenience, we screened ligands with $[Rh(C_2H_4)_2]_2$ instead of preparing and isolating each ligated rhodium complex. Interestingly, (*R*)-BINAP displayed higher enantioselectivities (49% *ee*) with this procedure compared to Hayashi's original report (entry 1). Other axially chiral bisphosphines such as (*R*)-SEGPHOS gave improved enantioselectivity but similarly poor yields (entry 2). Josiphos SL009, on the other hand, yielded **113** in 66% yield but in completely racemic form (entry 3). Alkyl bisphosphines such as (*S*,*S*)-DPP-pentane and (*R*,*R*)-Ph-BPE gave modest yields of **113** but significantly improved enantioselectivities for the opposite enantiomer (entries 4 and 5). Switching to the antipode, (*S*,*S*)-Ph-BPE, along with changing the method for arylzinc generation, successfully gave **113** in 60% yield and 99% *ee*.

With optimal conditions identified for the Rh-catalyzed enantioselective conjugate arylation of pyridone **111**, we aimed to intercept the racemic route to provide access to (−)-**2**. First, confirmation of the absolute configuration of **113** was achieved through derivatization to a crystalline ferrocenoyl piperidone (**114**), which displayed a Flack parameter near zero (Figure 10B). Alpha-methylation of pyridone with LiHMDS and MeOTf, followed by hydrogenolysis of the -CBz group, afforded piperidone **66** with minor loss of enantioenrichment (93% *ee*), which may be advanced further to obtain (−)-**2** through a 12-step enantioselective formal synthesis.

2.4.4. Complexity Analysis. In several instances, it proved necessary to install excess molecular complexity relative to the intended target, rendering bond cleavage steps as the strategic element of the overall transformations. Counterintuitively, these two-stage transformations challenge simplified complexity analysis wherein only reductions in structural complexity are considered, such as in MolComplex. The synthetic impact of these tactics with respect to complexity is illustrated with quantitative metrics for molecular complexity as developed by Krzyzanowski et al.[6] (Figure 11A). Most significant spikes in

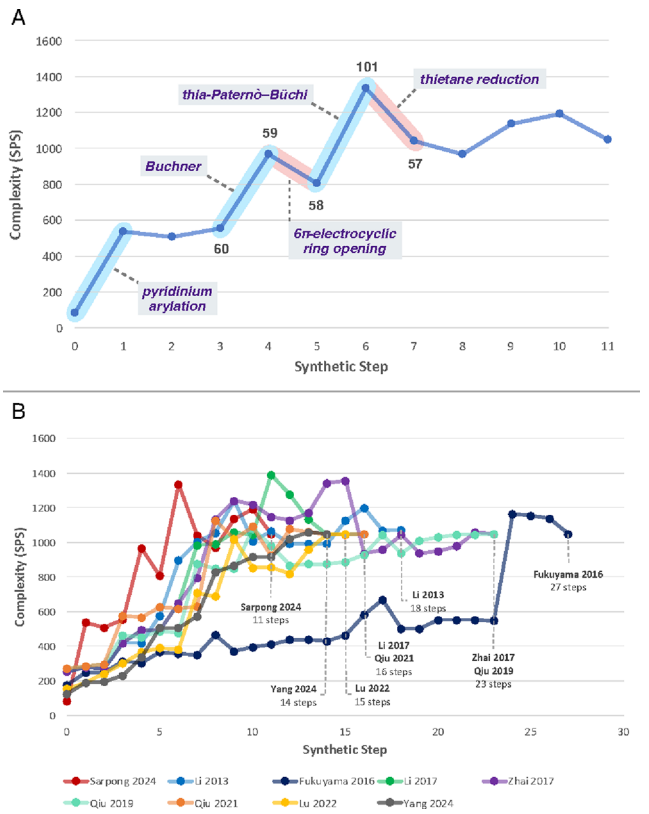

Figure 11. (A) Plot of molecular complexity (SPS score) of intermediates in our synthetic approach to daphenylline (**2**). Key C−C bond-forming steps highlighted in blue; bond-cleaving steps highlighted in pink. (B) Comparison of various synthetic approaches to **2**. See the Supporting Information for detailed analysis.

complexity (63% increase, **60** → **59**; 66% increase, **58** → **101**, blue highlights) were immediately coupled with a rapid drop in complexity (16% decrease, **59** → **58**; 22% decrease, **101** → **57**, pink highlights) through bond cleavage transformations. These short-term strategic concessions of excess structural complexity had immediate payoff, avoiding lengthy sequences of functional group interconversions that are often necessitated by complex, highly functionalized intermediates, as illustrated by several previous synthetic approaches to **2** (Figure 11B). Overall, navigation of this complexity space through drastic

https://doi.org/10.1021/jacs.4c11252
J. Am. Chem. Soc. 2024, 146, 33130−33148

C−C bond-forming and bond-cleaving transformations resulted in a highly efficient 11-step total synthesis of daphenylline (**2**), the shortest synthesis of **2** reported to date.

3. CONCLUSIONS

In this study, complexity analysis—either by MolComplex or network analysis—served as an inspirational starting point for the development of new synthetic strategies to **1** and **2**, two *Daphniphyllum* alkaloids. In the case of himalensine A (**1**), quantification of structural complexity and analysis of retrosynthetic precursors with MolComplex, a publicly accessible web application (www.molcomplex.org), led to the identification of transannular disconnections involving macrocyclic intermediates, both of which are underexplored in total synthesis. To this end, we prepared a key macrocyclic intermediate (**23**) and observed intriguing transannular reactivity in the formation of aza-bicyclo[3.3.1]nonane **33**. However, despite repeated attempts to form the desired transannular bond, the innate transannular reactivity of macrocycle **23** prevented this approach from ultimately advancing to **1**, underscoring the need for a hybrid approach in considering conformational subtleties alongside pure molecular graph-based retrosynthetic disconnections.

In a second case study, we completed a total synthesis of daphenylline (**2**) guided by a series of disconnections involving "excess complexity". In these two-stage transformations, a rapid buildup of structural complexity was coupled with a subsequent C−C bond cleavage step to access key intermediates, which would be challenging to prepare otherwise. In particular, [2 + 2] photocycloaddition with lactam **58** proved crucial to the installation of the quaternary methyl group, and a series of cyclobutanes and thietanes were prepared to explore this transformation. Completion of the total synthesis involved a variation on this theme: Friedel−Crafts cyclization of ketone **107**, followed by deoxygenation of the resulting bridgehead hydroxy group, gave daphenylline (**2**) in 11 total steps from commercially available starting materials. In light of these two distinct approaches to the complex *Daphniphyllum* alkaloids, we anticipate that complexity analysis will continue to inspire additional synthetic strategies to complex natural product targets.

■ ASSOCIATED CONTENT

Supporting Information

The Supporting Information is available free of charge at https://pubs.acs.org/doi/10.1021/jacs.4c11252.

Experimental procedures, spectroscopic data, and X-ray crystallographic data (PDF)

Accession Codes

CCDC 2334997−2335000 contain the supplementary crystallographic data for this paper. These data can be obtained free of charge via www.ccdc.cam.ac.uk/data_request/cif, or by emailing data_request@ccdc.cam.ac.uk, or by contacting The Cambridge Crystallographic Data Centre, 12 Union Road, Cambridge CB2 1EZ, UK; fax: +44 1223 336033.

■ AUTHOR INFORMATION

Corresponding Authors

Robert S. Paton − *Department of Chemistry, Colorado State University, Fort Collins, Colorado 80523, United States;* orcid.org/0000-0002-0104-4166; Email: robert.paton@colostate.edu

Richmond Sarpong − *Department of Chemistry, University of California, Berkeley, Berkeley, California 94720, United States;* orcid.org/0000-0002-0028-6323; Email: rsarpong@berkeley.edu

Authors

Brandon A. Wright − *Department of Chemistry, University of California, Berkeley, Berkeley, California 94720, United States;* orcid.org/0000-0003-4149-5292

Taku Okada − *Department of Chemistry, University of California, Berkeley, Berkeley, California 94720, United States;* orcid.org/0000-0002-0195-3335

Alessio Regni − *Department of Chemistry, University of California, Berkeley, Berkeley, California 94720, United States;* orcid.org/0000-0002-2188-1789

Guilian Luchini − *Department of Chemistry, Colorado State University, Fort Collins, Colorado 80523, United States;* orcid.org/0000-0003-0135-9624

Shree Sowndarya S. V − *Department of Chemistry, Colorado State University, Fort Collins, Colorado 80523, United States*

Nattawadee Chaisan − *Department of Chemistry, University of California, Berkeley, Berkeley, California 94720, United States*

Sebastian Kölbl − *Department of Chemistry, University of California, Berkeley, Berkeley, California 94720, United States*

Sojung F. Kim − *Department of Chemistry, University of California, Berkeley, Berkeley, California 94720, United States;* orcid.org/0000-0001-5089-8259

Complete contact information is available at: https://pubs.acs.org/10.1021/jacs.4c11252

Funding

Partial support of the work conducted at Berkeley was supported by the NSF CCAS (CHE-2202693) and NIGMS (R35 GM130345). B. A. W. is grateful to the National Science Foundation for a graduate fellowship (DGE-1106400) and UC Cancer Research Coordinating Committee for additional funding. T. O. acknowledges the Astellas Foundation for Research on Metabolic Disorders for funding. A. R. is grateful to the University of Urbino for funding. N. C. was supported by a fellowship from the National Research Council of Thailand (NRCT). S. F. K. was supported by the UC Berkeley Amgen Scholars program. R. S. P. thanks the Alpine high-performance computing resource, jointly funded by the University of Colorado Boulder, the University of Colorado Anschutz, and Colorado State University, and ACCESS through allocation TG-CHE180056 and CHE240020. We would also like to acknowledge the NSF Center for Computer-Assisted Synthesis (CCAS) for support.

Notes

The authors declare no competing financial interest.

■ ACKNOWLEDGMENTS

We thank Dr. Hasan Celik, Dr. Raynald Giovine, and the Pines Magnetic Resonance Center's Core NMR Facility (PMRC Core) at UC Berkeley. The instrument used in this work was in part supported by NIH S10OD024998. We also thank Drs. Ulla Andersen and Zongrui Zhou at the UC Berkeley QB3 Mass Spectrometry Facility for mass spectrometry analysis. We are also grateful to Dr. Nicholas Settineri (UC Berkeley) for X-ray crystallographic analysis.

REFERENCES

(1) Corey, E. J.; Cheng, X.-M. *The Logic of Chemical Synthesis*; John Wiley & Sons, Ltd.: 1996.
(2) Corey, E. J.; Wipke, W. T. Computer-Assisted Design of Complex Organic Syntheses. *Science* **1969**, *166* (3902), 178−192.
(3) Sheridan, R. P.; Zorn, N.; Sherer, E. C.; Campeau, L.-C.; Chang, C.; Cumming, J.; Maddess, M. L.; Nantermet, P. G.; Sinz, C. J.; O'Shea, P. D. Modeling a Crowdsourced Definition of Molecular Complexity. *J. Chem. Inf. Model.* **2014**, *54* (6), 1604−1616.
(4) Bertz, S. H. The First General Index of Molecular Complexity. *J. Am. Chem. Soc.* **1981**, *103* (12), 3599−3601.
(5) Böttcher, T. An Additive Definition of Molecular Complexity. *J. Chem. Inf. Model.* **2016**, *56* (3), 462−470.
(6) Krzyzanowski, A.; Pahl, A.; Grigalunas, M.; Waldmann, H. Spacial Score—A Comprehensive Topological Indicator for Small-Molecule Complexity. *J. Med. Chem.* **2023**, *66* (18), 12739−12750.
(7) Barone, R.; Chanon, M. A New and Simple Approach to Chemical Complexity. Application to the Synthesis of Natural Products. *J. Chem. Inf. Comput. Sci.* **2001**, *41* (2), 269−272.
(8) Demoret, R. M.; Baker, M. A.; Ohtawa, M.; Chen, S.; Lam, C. C.; Khom, S.; Roberto, M.; Forli, S.; Houk, K. N.; Shenvi, R. A. Synthetic, Mechanistic, and Biological Interrogation of Ginkgo Biloba Chemical Space En Route to (−)-Bilobalide. *J. Am. Chem. Soc.* **2020**, *142* (43), 18599−18618.
(9) Bertz, S. H.; Sommer, T. J. Rigorous Mathematical Approaches to Strategic Bonds and Synthetic Analysis Based on Conceptually Simple New Complexity Indices. *Chem. Commun.* **1997**, *16* (24), 2409−2410.
(10) Bertz, S.; Convergence, H. Molecular Complexity, and Synthetic Analysis. *J. Am. Chem. Soc.* **1982**, *104* (21), 5801−5803.
(11) Marth, C. J.; Gallego, G. M.; Lee, J. C.; Lebold, T. P.; Kulyk, S.; Kou, K. G. M.; Qin, J.; Lilien, R.; Sarpong, R. Network-Analysis-Guided Synthesis of Weisaconitine D and Liljestrandinine. *Nature* **2015**, *528* (7583), 493−498.
(12) Doering, N. A.; Sarpong, R.; Hoffmann, R. W. A Case for Bond-Network Analysis in the Synthesis of Bridged Polycyclic Complex Molecules: Hetidine and Hetisine Diterpenoid Alkaloids. *Angew. Chem., Int. Ed.* **2020**, *59* (27), 10722−10731.
(13) Owens, K. R.; McCowen, S. V.; Blackford, K. A.; Ueno, S.; Hirooka, Y.; Weber, M.; Sarpong, R. Total Synthesis of the Diterpenoid Alkaloid Arcutinidine Using a Strategy Inspired by Chemical Network Analysis. *J. Am. Chem. Soc.* **2019**, *141* (35), 13713−13717.
(14) Haider, M.; Sennari, G.; Eggert, A.; Sarpong, R. Total Synthesis of the Cephalotaxus Norditerpenoids (±)-Cephanolides A−D. *J. Am. Chem. Soc.* **2021**, *143* (7), 2710−2715.
(15) Lusi, R. F.; Sennari, G.; Sarpong, R. Total Synthesis of Nine Longiborneol Sesquiterpenoids Using a Functionalized Camphor Strategy. *Nat. Chem.* **2022**, *14* (4), 450−456.
(16) Blume, C. Daphniphyllum. *Bijdr. Fl. Ned. Ind.* **1826**, *17*, 1152−1153.
(17) Kobayashi, J.; Kubota, T. The Daphniphyllum Alkaloids. *Nat. Prod. Rep.* **2009**, *26* (7), 936−962.
(18) Heathcock, C. H. The Enchanting Alkaloids of Yuzuriha. *Angew. Chem., Int. Ed. Engl.* **1992**, *31* (6), 665−681.
(19) Chattopadhyay, A. K.; Hanessian, S. Recent Progress in the Chemistry of Daphniphyllum Alkaloids. *Chem. Rev.* **2017**, *117* (5), 4104−4146.
(20) Kobayashi, J. I.; Morita, H. The daphniphyllum alkaloids. In *The Alkaloids: Chemistry and Biology*; Academic Press: 2003, Vol. *60*, pp 165−205. .
(21) Ruggeri, R. B.; Heathcock, C. H. Daphniphyllum Alkaloids. Part 7. Biomimetic Total Synthesis of (.+-.)-Methyl Homodaphniphyllate. *J. Org. Chem.* **1990**, *55* (12), 3714−3715.
(22) Piettre, S.; Heathcock, C. H. Biomimetic Total Synthesis of Proto-Daphniphylline. *Science* **1990**, *248* (4962), 1532−1534.
(23) Heathcock, C. H. Nature Knows Best: An Amazing Reaction Cascade Is Uncovered by Design and Discovery. *Proc. Natl. Acad. Sci. U. S. A.* **1996**, *93* (25), 14323−14327.
(24) Weiss, M. E.; Carreira, E. M. Total Synthesis of (+)-Daphmanidin E. *Angew. Chem., Int. Ed.* **2011**, *50* (48), 11501−11505.
(25) Shvartsbart, A.; Smith, A. B. I. The Daphniphyllum Alkaloids: Total Synthesis of (−)-Calyciphylline N. *J. Am. Chem. Soc.* **2015**, *137* (10), 3510−3519.
(26) Shvartsbart, A.; Smith, A. B. I. Total Synthesis of (−)-Calyciphylline N. *J. Am. Chem. Soc.* **2014**, *136* (3), 870−873.
(27) Chattopadhyay, A. K.; Ly, V. L.; Jakkepally, S.; Berger, G.; Hanessian, S. Total Synthesis of Isodaphlongamine H: A Possible Biogenetic Conundrum. *Angew. Chem., Int. Ed.* **2016**, *55* (7), 2577−2581.
(28) Lu, Z.; Li, Y.; Deng, J.; Li, A. Total Synthesis of the Daphniphyllum Alkaloid Daphenylline. *Nat. Chem.* **2013**, *5* (8), 679−684.
(29) Zhang, W.; Lu, M.; Ren, L.; Zhang, X.; Liu, S.; Ba, M.; Yang, P.; Li, A. Total Synthesis of Four Classes of Daphniphyllum Alkaloids. *J. Am. Chem. Soc.* **2023**, *145* (49), 26569−26579.
(30) Yamada, R.; Adachi, Y.; Yokoshima, S.; Fukuyama, T. Total Synthesis of (−)-Daphenylline. *Angew. Chem., Int. Ed.* **2016**, *55* (20), 6067−6070.
(31) Shi, H.; Michaelides, I. N.; Darses, B.; Jakubec, P.; Nguyen, Q. N. N.; Paton, R. S.; Dixon, D. J. Total Synthesis of (−)-Himalensine A. *J. Am. Chem. Soc.* **2017**, *139* (49), 17755−17758.
(32) Kučera, R.; Ellis, S. R.; Yamazaki, K.; Hayward Cooke, J.; Chekshin, N.; Christensen, K. E.; Hamlin, T. A.; Dixon, D. J. Enantioselective Total Synthesis of (−)-Himalensine A via a Palladium and 4-Hydroxyproline Co-Catalyzed Desymmetrization of Vinyl-Bromide-Tethered Cyclohexanones. *J. Am. Chem. Soc.* **2023**, *145* (9), 5422−5430.
(33) Chen, Y.; Hu, J.; Guo, L.-D.; Zhong, W.; Ning, C.; Xu, J. A Concise Total Synthesis of (−)-Himalensine A. *Angew. Chem., Int. Ed.* **2019**, *58* (22), 7390−7394.
(34) Guo, L.-D.; Chen, Y.; Xu, J. Total Synthesis of Daphniphyllum Alkaloids: From Bicycles to Diversified Caged Structures. *Acc. Chem. Res.* **2020**, *53* (11), 2726−2737.
(35) Guo, L.-D.; Zhang, Y.; Hu, J.; Ning, C.; Fu, H.; Chen, Y.; Xu, J. Asymmetric Total Synthesis of Yuzurimine-Type Daphniphyllum Alkaloid (+)-Caldaphnidine J. *Nat. Commun.* **2020**, *11* (1), 3538.
(36) Chen, X.; Zhang, H.-J.; Yang, X.; Lv, H.; Shao, X.; Tao, C.; Wang, H.; Cheng, B.; Li, Y.; Guo, J.; Zhang, J.; Zhai, H. Divergent Total Syntheses of (−)-Daphnilongeranin B and (−)-Daphenylline. *Angew. Chem., Int. Ed.* **2018**, *57* (4), 947−951.
(37) Xu, G.; Wu, J.; Li, L.; Lu, Y.; Li, C. Total Synthesis of (−)-Daphnezomines A and B. *J. Am. Chem. Soc.* **2020**, *142* (36), 15240−15245.
(38) Li, L.-X.; Min, L.; Yao, T.-B.; Ji, S.-X.; Qiao, C.; Tian, P.-L.; Sun, J.; Li, C.-C. Total Synthesis of Yuzurine-Type Alkaloid Daphgraciline. *J. Am. Chem. Soc.* **2022**, *144* (41), 18823−18828.
(39) Zou, Y.-P.; Lai, Z.-L.; Zhang, M.-W.; Peng, J.; Ning, S.; Li, C.-C. Total Synthesis of (±)- and (−)-Daphnillonin B. *J. Am. Chem. Soc.* **2023**, *145* (20), 10998−11004.
(40) Cao, M.-Y.; Ma, B.-J.; Gu, Q.-X.; Fu, B.; Lu, H.-H. Concise Enantioselective Total Synthesis of Daphenylline Enabled by an Intramolecular Oxidative Dearomatization. *J. Am. Chem. Soc.* **2022**, *144* (13), 5750−5755.
(41) Wu, B.-L.; Yao, J.-N.; Long, X.-X.; Tan, Z.-Q.; Liang, X.; Feng, L.; Wei, K.; Yang, Y.-R. Enantioselective Total Synthesis of (−)-Daphenylline. *J. Am. Chem. Soc.* **2024**, *146* (2), 1262−1268.
(42) Hugelshofer, C. L.; Palani, V.; Sarpong, R. Calyciphylline B-Type Alkaloids: Total Syntheses of (−)-Daphlongamine H and (−)-Isodaphlongamine H. *J. Am. Chem. Soc.* **2019**, *141* (21), 8431−8435.
(43) Hugelshofer, C. L.; Palani, V.; Sarpong, R. Calyciphylline B-Type Alkaloids: Evolution of a Synthetic Strategy to (−)-Daphlongamine H. *J. Org. Chem.* **2019**, *84* (21), 14069−14091.
(44) Wright, B. A.; Regni, A.; Chaisan, N.; Sarpong, R. Navigating Excess Complexity: Total Synthesis of Daphenylline. *J. Am. Chem. Soc.* **2024**, *146* (3), 1813−1818.

https://doi.org/10.1021/jacs.4c11252
J. Am. Chem. Soc. 2024, 146, 33130−33148

(45) Morita, H.; Kobayashi, J. Calyciphyllines A and B, Two Novel Hexacyclic Alkaloids from Daphniphyllum Calycinum. *Org. Lett.* **2003**, *5* (16), 2895−2898.
(46) Kang, B.; Jakubec, P.; Dixon, D. J. Strategies towards the Synthesis of Calyciphylline A-Type Daphniphyllum Alkaloids. *Nat. Prod. Rep.* **2014**, *31* (4), 550−562.
(47) Zhang, H.; Shyaula, S. L.; Li, J.-Y.; Li, J.; Yue, J.-M. Himalensines A and B, Alkaloids from Daphniphyllum Himalense. *Org. Lett.* **2016**, *18* (5), 1202−1205.
(48) Zhang, Q.; Di, Y.-T.; Li, C.-S.; Fang, X.; Tan, C.-J.; Zhang, Z.; Zhang, Y.; He, H.-P.; Li, S.-L.; Hao, X.-J. Daphenylline, a New Alkaloid with an Unusual Skeleton, from Daphniphyllum Longeracemosum. *Org. Lett.* **2009**, *11* (11), 2357−2359.
(49) Yang, S.-P.; Zhang, H.; Zhang, C.-R.; Cheng, H.-D.; Yue, J.-M. Alkaloids from Daphniphyllum Longeracemosum. *J. Nat. Prod.* **2006**, *69* (1), 79−82.
(50) Zhang, H.; Shyaula, S. L.; Li, J. Y.; Li, J.; Yue, J. M. Hydroxylated Daphniphyllum Alkaloids from Daphniphyllum Himalense. *J. Nat. Prod.* **2015**, *78* (11), 2761−2767.
(51) Zhong, J.; Chen, K.; Qiu, Y.; He, H.; Gao, S. A Unified Strategy to Construct the Tetracyclic Ring of Calyciphylline A Alkaloids: Total Synthesis of Himalensine A. *Org. Lett.* **2019**, *21* (10), 3741−3745.
(52) Chen, Y.; Zhang, W.; Ren, L.; Li, J.; Li, A. Total Syntheses of Daphenylline, Daphnipaxianine A, and Himalenine D. *Angew. Chem., Int. Ed.* **2018**, *57* (4), 952−956.
(53) Herzon, S. B. Emergent Properties of Natural Products. *Synlett* **2018**, *29* (14), 1823−1835.
(54) Saridakis, I.; Kaiser, D.; Maulide, N. Unconventional Macrocyclizations in Natural Product Synthesis. *ACS Cent. Sci.* **2020**, *6* (11), 1869−1889.
(55) Zheng, K.; Hong, R. Stereoconfining Macrocyclizations in the Total Synthesis of Natural Products. *Nat. Prod. Rep.* **2019**, *36* (11), 1546−1575.
(56) Fürstner, A. Lessons from Natural Product Total Synthesis: Macrocyclization and Postcyclization Strategies. *Acc. Chem. Res.* **2021**, *54* (4), 861−874.
(57) Vosburg, D. A.; Vanderwal, C. D.; Sorensen, E. J. A Synthesis of (+)-FR182877, Featuring Tandem Transannular Diels−Alder Reactions Inspired by a Postulated Biogenesis. *J. Am. Chem. Soc.* **2002**, *124* (17), 4552−4553.
(58) Evans, D. A.; Starr, J. T. A Cascade Cycloaddition Strategy Leading to the Total Synthesis of (−)-FR182877. *Angew. Chem., Int. Ed.* **2002**, *41* (10), 1787−1790.
(59) Kuroda, Y.; Nicacio, K. J.; Da Silva, I. A. Jr.; Leger, P. R.; Chang, S.; Gubiani, J. R.; Deflon, V. M.; Nagashima, N.; Rode, A.; Blackford, K.; Ferreira, A. G.; Sette, L. D.; Williams, D. E.; Andersen, R. J.; Jancar, S.; Berlinck, R. G. S.; Sarpong, R. Isolation, Synthesis and Bioactivity Studies of Phomactin Terpenoids. *Nat. Chem.* **2018**, *10* (9), 938−945.
(60) Lo, J. C.; Kim, D.; Pan, C.-M.; Edwards, J. T.; Yabe, Y.; Gui, J.; Qin, T.; Gutiérrez, S.; Giacoboni, J.; Smith, M. W.; Holland, P. L.; Baran, P. S. Fe-Catalyzed C−C Bond Construction from Olefins via Radicals. *J. Am. Chem. Soc.* **2017**, *139* (6), 2484−2503.
(61) Corminboeuf, O.; Overman, L. E.; Pennington, L. D. Enantioselective Total Synthesis of Briarellins E and F: The First Total Syntheses of Briarellin Diterpenes. *J. Am. Chem. Soc.* **2003**, *125* (22), 6650−6652.
(62) Corminboeuf, O.; Overman, L. E.; Pennington, L. D. A Unified Strategy for Enantioselective Total Synthesis of Cladiellin and Briarellin Diterpenes: Total Synthesis of Briarellins E and F and the Putative Structure of Alcyonin and Revision of Its Structure Assignment. *J. Org. Chem.* **2009**, *74* (15), 5458−5470.
(63) Jang, W. J.; Song, S. M.; Moon, J. H.; Lee, J. Y.; Yun, J. Copper-Catalyzed Enantioselective Hydroboration of Unactivated 1, 1-Disubstituted Alkenes. *J. Am. Chem. Soc.* **2017**, *139* (39), 13660−13663.
(64) Comins, D. L.; Dehghani, A. Pyridine-Derived Triflating Reagents: An Improved Preparation of Vinyl Triflates from Metallo Enolates. *Tetrahedron Lett.* **1992**, *33* (42), 6299−6302.
(65) Xi, Y.; Hartwig, J. F. Mechanistic Studies of Copper-Catalyzed Asymmetric Hydroboration of Alkenes. *J. Am. Chem. Soc.* **2017**, *139* (36), 12758−12772.
(66) Takagi, J.; Takahashi, K.; Ishiyama, T.; Miyaura, N. Palladium-Catalyzed Cross-Coupling Reaction of Bis (Pinacolato) Diboron with 1-Alkenyl Halides or Triflates: Convenient Synthesis of Unsymmetrical 1, 3-Dienes via the Borylation-Coupling Sequence. *J. Am. Chem. Soc.* **2002**, *124* (27), 8001−8006.
(67) Beaulieu, P. *Approach to the Synthesis of Spiroiridal-Type Triterpenoids via an Ireland-Claisen Rearrangement*; University of Ottawa: 2004.
(68) Chatterjee, A. K.; Choi, T.-L.; Sanders, D. P.; Grubbs, R. H. A General Model for Selectivity in Olefin Cross Metathesis. *J. Am. Chem. Soc.* **2003**, *125* (37), 11360−11370.
(69) Lipshutz, B. H.; Noson, K.; Chrisman, W.; Lower, A. Asymmetric Hydrosilylation of Aryl Ketones Catalyzed by Copper Hydride Complexed by Nonracemic Biphenyl Bis-Phosphine Ligands. *J. Am. Chem. Soc.* **2003**, *125* (29), 8779−8789.
(70) Johnson, C. R.; Adams, J. P.; Braun, M. P.; Senanayake, C. B. W.; Wovkulich, P. M.; Uskoković, M. R. Direct α-Iodination of Cycloalkenones. *Tetrahedron Lett.* **1992**, *33* (7), 917−918.
(71) Uenishi, J.; Beau, J. M.; Armstrong, R. W.; Kishi, Y. Dramatic Rate Enhancement of Suzuki Diene Synthesis. Its Application to Palytoxin Synthesis. *J. Am. Chem. Soc.* **1987**, *109* (15), 4756−4758.
(72) Weitz, E.; Scheffer, A. Über Die Einwirkung von Alkalischem Wasserstoffsuperoxyd Auf Ungesättigte Verbindungen. *Berichte Dtsch. Chem. Ges. B Ser.* **1921**, *54* (9), 2327−2344.
(73) Dubovyk, I.; Watson, I. D. G.; Yudin, A. K. Achieving Control over the Branched/Linear Selectivity in Palladium-Catalyzed Allylic Amination. *J. Org. Chem.* **2013**, *78* (4), 1559−1575.
(74) Mikan, C. P.; Matthews, A.; Harris, D.; McIvor, C. E.; Waddell, P. G.; Sims, M. T.; Knowles, J. P. Stereoselective Two-Carbon Ring Expansion of Allylic Amines via Electronic Control of Palladium-Promoted Equilibria. *Chem. Sci.* **2023**, *14* (25), 6992−6996.
(75) Kornblum, N.; DeLaMare, H. E. The Base Catalyzed Decomposition of a Dialkyl Peroxide. *J. Am. Chem. Soc.* **1951**, *73* (2), 880−881.
(76) Holstein, P. M.; Holstein, J. J.; Escudero-Adán, E. C.; Baudoin, O.; Echavarren, A. M. Ferrocene Derivatives of Liquid Chiral Molecules Allow Assignment of Absolute Configuration by X-Ray Crystallography. *Howard Flack Meml. Issue 1943 - 2017* **2017**, *28* (10), 1321−1329.
(77) Sutbeyaz, Y.; Secen, H.; Balci, M. Cobalt(II) Tetraphenylporphyrin-Catalyzed Decomposition of Bicyclic Endoperoxides. *J. Org. Chem.* **1988**, *53* (10), 2312−2317.
(78) Siddiqi, Z. R.; Ungarean, C. N.; Bingham, T. W.; Sarlah, D. Development of a Scalable and Sublimation-Free Route to MTAD. *Org. Process Res. Dev.* **2020**, *24* (12), 2953−2959.
(79) Tang, C.; Okumura, M.; Deng, H.; Sarlah, D. Palladium-Catalyzed Dearomative Syn-1,4-Oxyamination. *Angew. Chem., Int. Ed.* **2019**, *58* (44), 15762−15766.
(80) Farney, E. P.; Feng, S. S.; Schäfers, F.; Reisman, S. E. Total Synthesis of (+)-Pleuromutilin. *J. Am. Chem. Soc.* **2018**, *140* (4), 1267−1270.
(81) Breunig, M.; Yuan, P.; Gaich, T. An Unexpected Transannular [4 + 2] Cycloaddition during the Total Synthesis of (+)-Norcembrene 5. *Angew. Chem., Int. Ed.* **2020**, *59* (14), 5521−5525.
(82) Perea, M. A.; Wang, B.; Wyler, B. C.; Ham, J. S.; O'Connor, N. R.; Nagasawa, S.; Kimura, Y.; Manske, C.; Scherübl, M.; Nguyen, J. M.; Sarpong, R. General Synthetic Approach to Diverse Taxane Cores. *J. Am. Chem. Soc.* **2022**, *144* (46), 21398−21407.
(83) Xu, B.; Wang, B.; Xun, W.; Qiu, F. G. Total Synthesis of (−)-Daphenylline. *Angew. Chem., Int. Ed.* **2019**, *58* (17), 5754−5757.
(84) Wang, B.; Xu, B.; Xun, W.; Guo, Y.; Zhang, J.; Qiu, F. G. A General Strategy for the Construction of Calyciphylline A-Type Alkaloids: Divergent Total Syntheses of (−)-Daphenylline and (−)-Himalensine A. *Angew. Chem., Int. Ed.* **2021**, *60* (17), 9439−9443.

https://doi.org/10.1021/jacs.4c11252
J. Am. Chem. Soc. 2024, 146, 33130−33148

(85) Hoffmann, R. W. *Elements of Synthesis Planning*; Springer: Heidelberg, 2009.
(86) Cherney, E. C.; Green, J. C.; Baran, P. S. Synthesis of Ent-Kaurane and Beyerane Diterpenoids by Controlled Fragmentations of Overbred Intermediates. *Angew. Chem., Int. Ed.* **2013**, *52* (34), 9019−9022.
(87) Chen, H.; Li, Z.; Shao, P.; Yuan, H.; Chen, S.-C.; Luo, T. Total Synthesis of (+)-Mutilin: A Transannular [2 + 2] Cycloaddition/Fragmentation Approach. *J. Am. Chem. Soc.* **2022**, *144* (34), 15462−15467.
(88) Xu, B.; Zhang, Z.; Tantillo, D. J.; Dai, M. Concise Total Syntheses of (−)-Crinipellins A and B Enabled by a Controlled Cargill Rearrangement. *J. Am. Chem. Soc.* **2024**, *146* (31), 21250−21256.
(89) Nandy, M.; Das, S.; Nanda, S. Cyclobutane Based "Overbred Intermediates" and Their Exploration in Organic Synthesis. *Org. Biomol. Chem.* **2022**, *20* (8), 1582−1622.
(90) Corey, E. J.; Howe, W. J.; Orf, H. W.; Pensak, D. A.; Petersson, G. General Methods of Synthetic Analysis. Strategic Bond Disconnections for Bridged Polycyclic Structures. *J. Am. Chem. Soc.* **1975**, *97* (21), 6116−6124.
(91) Huisgen, R.; Juppe, G. Benzo-Norcaradien-Carbonsäure Und Benzo-Cycloheptatrien-Carbonsäure. *Chem. Ber.* **1961**, *94* (8), 2332−2349.
(92) Frey, B.; Wells, A. P.; Rogers, D. H.; Mander, L. N. Synthesis of the Unusual Diterpenoid Tropones Hainanolidol and Harringtonolide. *J. Am. Chem. Soc.* **1998**, *120* (8), 1914−1915.
(93) Jones, D. W. Thermal Rearrangements of Benzobicyclononatrienes (1,4-Propeno-1,4-Dihydronaphthalenes) to Benzobarbaralanes; Intramolecular Diels−Alder Rather than Intramolecular Ene Reactions. *J. Chem. Soc. Chem. Commun.* **1989**, *19*, 1481−1483.
(94) Reisman, S. E.; Nani, R. R.; Levin, S. Buchner and Beyond: Arene Cyclopropanation as Applied to Natural Product Total Synthesis. *Synlett* **2011**, *2011* (17), 2437−2442.
(95) Xie, C.; Runnegar, M. T. C.; Snider, B. B. Total Synthesis of (±)-Cylindrospermopsin. *J. Am. Chem. Soc.* **2000**, *122* (21), 5017−5024.
(96) Comins, D. L.; Brooks, C. A.; Ingalls, C. L. Reduction of N-Acyl-2,3-Dihydro-4-Pyridones to N-Acyl-4-Piperidones Using Zinc/Acetic Acid. *J. Org. Chem.* **2001**, *66* (6), 2181−2182.
(97) Toma, T.; Shimokawa, J.; Fukuyama, T. N,N′-Ditosylhydrazine: A Convenient Reagent for Facile Synthesis of Diazoacetates. *Org. Lett.* **2007**, *9* (16), 3195−3197.
(98) Kaupang, Å.; Bonge-Hansen, T. α-Bromodiazoacetamides−a New Class of Diazo Compounds for Catalyst-Free, Ambient Temperature Intramolecular C−H Insertion Reactions. *Beilstein J. Org. Chem.* **2013**, *9* (1), 1407−1413.
(99) Zeng, Q.; Dong, K.; Pei, C.; Dong, S.; Hu, W.; Qiu, L.; Xu, X. Divergent Construction of Macrocyclic Alkynes via Catalytic Metal Carbene C(Sp2)−H Insertion and the Buchner Reaction. *ACS Catal.* **2019**, *9* (12), 10773−10779.
(100) Chen, K.; Kang, Q.-K.; Li, Y.; Wu, W.-Q.; Zhu, H.; Shi, H. Catalytic Amination of Phenols with Amines. *J. Am. Chem. Soc.* **2022**, *144* (3), 1144−1151.
(101) Southgate, E. H.; Pospech, J.; Fu, J.; Holycross, D. R.; Sarlah, D. Dearomative Dihydroxylation with Arenophiles. *Nat. Chem.* **2016**, *8* (10), 922−928.
(102) Leibler, I. N.-M.; Tekle-Smith, M. A.; Doyle, A. G. A General Strategy for C(Sp3)−H Functionalization with Nucleophiles Using Methyl Radical as a Hydrogen Atom Abstractor. *Nat. Commun.* **2021**, *12* (1), 6950.
(103) Padwa, A.; Jacquez, M. N.; Schmidt, A. An Approach toward Azacycles Using Photochemical and Radical Cyclizations of N-Alkenyl Substituted 5-Thioxopyrrolidin-2-Ones. *J. Org. Chem.* **2004**, *69* (1), 33−45.
(104) He, J.; Bai, Z.-Q.; Yuan, P.-F.; Wu, L.-Z.; Liu, Q. Highly Efficient Iridium-Based Photosensitizers for Thia-Paternò−Büchi Reaction and Aza-Photocyclization. *ACS Catal.* **2021**, *11* (1), 446−455.
(105) Hauptmann, H.; Walter, W. F. The Action of Raney Nickel on Organic Sulfur Compounds. *Chem. Rev.* **1962**, *62* (5), 347−404.
(106) Hill, R. R.; Rychnovsky, S. D. Generation, Stability, and Utility of Lithium 4,4′-Di-Tert-Butylbiphenylide (LiDBB). *J. Org. Chem.* **2016**, *81* (22), 10707−10714.
(107) Fieser, L. F.; Fieser, M.*Reagents for Organic Synthesis*; John Wiley & Sons, Ltd.: 1967.
(108) Comins, D. L.; Zhang, Y.; Joseph, S. P. Enantiopure N-Acyldihydropyridones as Synthetic Intermediates: Asymmetric Synthesis of Benzomorphans. *Org. Lett.* **1999**, *1* (4), 657−660.
(109) Eaton, P. E.; Carlson, G. R.; Lee, J. T. Phosphorus Pentoxide-Methanesulfonic Acid. Convenient Alternative to Polyphosphoric Acid. *J. Org. Chem.* **1973**, *38* (23), 4071−4073.
(110) Dolan, S. C.; MacMillan, J. A New Method for the Deoxygenation of Tertiary and Secondary Alcohols. *J. Chem. Soc. Chem. Commun.* **1985**, *22*, 1588−1589.
(111) Shintani, R.; Tokunaga, N.; Doi, H.; Hayashi, T. A New Entry of Nucleophiles in Rhodium-Catalyzed Asymmetric 1,4-Addition Reactions: Addition of Organozinc Reagents for the Synthesis of 2-Aryl-4-Piperidones. *J. Am. Chem. Soc.* **2004**, *126* (20), 6240−6241.

https://doi.org/10.1021/jacs.4c11252
J. Am. Chem. Soc. 2024, 146, 33130−33148